Article

Title: Controlled Release of H_2S and NO through Air-Stimulated Anion Exchange

Authors: Shinsuke Ishihara* and Nobuo Iyi*

Affiliation: International Center for Materials Nanoarchitectonics (WPI-MANA), National Institute for Materials Science (NIMS), 1-1 Namiki, Tsukuba, Ibaraki 305-0044, Japan

*Corresponding author.
Email: ISHIHARA.Shinsuke@nims.go.jp, IYI.Nobuo@nims.go.jp

Abstract: H_2S and NO are gas molecules with physiological activities; solid materials that release these gases under safe and ubiquitous stimuli offer broad medical applications. Herein, we report solid materials that autonomously release ppm-level H_2S or NO under air. HS^- or NO_2^- incorporated in the interlayer of layered double hydroxide (LDH), a clay mineral, is protonated by CO_2 and H_2O, yielding H_2S or HNO_2. HNO_2 generates NO through disproportionation or reduction. Moreover, another NO-release method employs solid mixtures of NO_2^--incorporated LDH and $FeSO_4$, wherein wet air triggers NO_2^- reduction with Fe^{2+} through anion exchange between NO_2^- and SO_4^{2-}. A potential application of the air-stimulated gas release system is demonstrated by creating a portable and battery-free NO inhaler for emergency treatment of respiratory distress.

One Sentence Summary: Solid materials that release ppm-level H_2S and NO in response to CO_2 and H_2O broaden medical applications of these physiologically active gases.

Keywords: hydrogen sulfide, nitric oxide, physiologically active gases, controlled release, layered double hydroxide, anion exchange

MAIN TEXT:

INTRODUCTION

Gas molecules play key roles in versatile research fields, and their practical utility depends on safety and cost-effectivity in the gas delivery system.[1–3] The use of high-pressure gas cylinders often causes safety concerns; therefore, solid materials that release gas molecules under external stimuli (e.g., heat, light, and pressure) attract particular interest.[4,5] H_2S and NO, which are widely known as toxic and labile gases, show unique physiological activities (e.g., anti-inflammatory, anti-oxidation, cytoprotection, vasodilation) at ppm-level concentration.[6–8] However, due to the lack of a reliable delivery system, the medical application of H_2S (in gaseous form) is not practical at present (except for a folk remedy at sulfurous spring[9]). Besides, NO becomes a selective and fast-acting pulmonary vasodilator upon inhalation, and inhaled-NO is a well-established method for treating respiratory distress such as persistent pulmonary hypertension of the newborn.[10–12] However, inhaled-NO requires a high-pressure gas cylinder, expensive medical instrument, and trained operator for controlling/monitoring the purity and dose of NO, which limit the broad adoption of the inhaled-NO technique in developing countries and outside hospital.[12–14]

Layered double hydroxides (LDHs) are inorganic layered materials with general formula $M^{II}_yM^{III}(OH)_{2(y+1)}(X^{n-})_{1/n}\cdot mH_2O$, where M^{II}, M^{III}, X^{n-}, and mH_2O are, respectively, a divalent metal cation (y is in the range 2−4), a trivalent metal cation, an n-valent anion, and hydrated water (m depends on humidity in environment) (Fig. 1A).[15] $M^{II}_yM^{III}(OH)_{2(y+1)}$ forms a positively charged 2D layer, and both charge-compensating anion (X^{n-}) and hydrated water (mH_2O) are located within the interlayer. Previously, we have reported that some anions (e.g., acetate and carbonate) in the interlayer of Mg/Al-type LDHs tend to exchange with CO_3^{2-} derived from aerial CO_2.[16–18] The anion-exchange phenomenon at the air−solid interface inspired us to explore a novel class of gas-releasing materials. Namely, we hypothesized that interlayer HS^- or NO_2^- in LDHs can be exchanged with aerial CO_2, resulting in autonomous release of H_2S or HNO_2 under air (Fig. 1A).

Herein, we report solid materials that autonomously release H_2S or HNO_2 in response to air (Fig. 1A, B). HNO_2 is convertible to NO through an automatic disproportionation reaction or subsequent treatment with a reducing agent (Fig. 1C).[19] Profiles of gas release, including concentration and duration, can be controlled by various factors such as chemical composition of LDHs, diffusion of gases and ions, and chemical equilibrium. The low-cost and safe-to-handle materials are feasible for creating a disposable system for a controlled release of ppm-level physiologically active gases. Use of air as the stimulus for gas release is advantageous in that air is safe, charge-free, and available anytime anywhere. The potential utility of our system is demonstrated by creating a portable and battery-free respirator that can supply therapeutically useful quantity of NO into inhaled air.

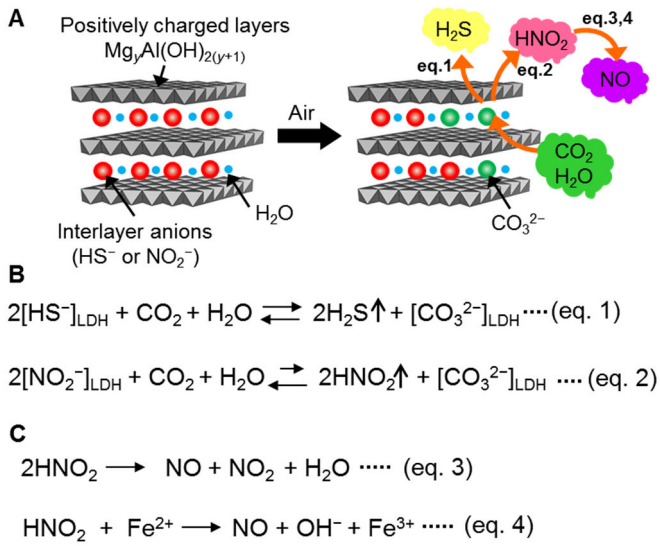

Fig. 1. Design of solid materials that release H_2S and NO gases in response to air. (**A**) Release of H_2S or HNO_2 from LDHs through anion exchange between interlayer anions (HS^- or NO_2^-) and aerial components (CO_2 and H_2O). (**B**) Protonation of interlayer anions with aerial components, yielding H_2S or HNO_2. (**C**) Disproportionation (eq. 3) or reduction (eq. 4) of HNO_2, yielding NO.

RESULTS AND DISCUSSION

Synthesis and characterization of H_2S-releasing LDHs.

LDHs involving HS^- or S^{2-}, for H_2S release, were synthesized by two-step anion exchange reactions.[20] As starting materials, CO_3^{2-}-type LDHs with Mg:Al ratio of 3:1 ($Mg_3Al(OH)_8(CO_3^{2-})_{0.5}\cdot 2H_2O$) and 2:1 ($Mg_2Al(OH)_6(CO_3^{2-})_{0.5}\cdot 2H_2O$) were utilized. The former is commercially available, and the latter was synthesized by a hydrothermal reaction.[21] As CO_3^{2-} of LDH is hardly exchangeable with other anions under mild conditions, CO_3^{2-} was first replaced with Cl^-.[22] Then, Cl^--type LDHs (Mg:Al = 2:1 or 3:1) dispersed in degassed deionized water were reacted with 10 equivalent (in mole) of $NaHS\cdot nH_2O$ or $Na_2S\cdot 9H_2O$ for 2 days under N_2, as summarized in Table S1. Solid materials were collected by filtration, washed with degassed deionized water, and then dried in vacuum (all performed under N_2 atmosphere) to afford four types of products (NaHS-Mg/Al(2/1), NaHS-Mg/Al(3/1), Na_2S-Mg/Al(2/1), and Na_2S-Mg/Al(3/1); see Fig. 2A for a typical image). The products were preserved in a sealed pack for isolation from air (Fig. S1). As far as we know, HS^-- or S^{2-}-incorporated LDHs, which are produced in an inert atmosphere throughout syntheses and preservation, have not been reported, though there are some examples synthesized and/or preserved under air.[23,24] A scanning electron microscopy (SEM) image showed that the morphology (hexagonal plate) of LDH was maintained after multi-step anion-exchange reactions (Fig. 2B).

NaHS-Mg/Al(2/1) released odor characteristic to H_2S for over 1 h when exposed to air **[CAUTION!!]**, and the response of the detector tube was positive (Fig. 2C). In addition, the released

gas was confirmed as H_2S through the formation of PbS upon interaction with Pb^{2+} (Fig. 2D). Moreover, SO_2 was not detected (<0.01 ppm) in ~10 ppm H_2S by the detector tube. The concentration of H_2S released from LDHs was continuously monitored by an electrochemical sensor under the standard flow conditions employed in this study (air, 50% relative humidity (RH), 100 mL/min, 20 °C), and NaHS-Mg/Al(2/1) demonstrated a rather steady release of ~10 ppm H_2S for 2 h (Fig. 2E). On the other hand, Na_2S-Mg/Al(2/1) did not release H_2S. NaHS-Mg/Al(3/1) and Na_2S-Mg/Al(3/1) released concentrated (over 25 ppm) H_2S, but the release profile was not as steady as that of NaHS-Mg/Al(2/1). A steady release profile of NaHS-Mg/Al(2/1) can be explained by a narrow interlayer distance of Mg/Al = 2/1-type LDHs,[18] which suppresses the interaction between interlayer anions and aerial components.

Thermogravimetry-differential thermal analysis (TG-DTA) showed that NaHS-Mg/Al(2/1) involves HS^- that demonstrate exothermal oxidation into $S_2O_3^{2-}$ at around 65−100 °C in air (Fig. 2F).[23,24] In contrast, exothermal signals were not observed for Na_2S-Mg/Al(2/1) at 65−100 °C, indicating that sulfur sources were not incorporated (Fig. S2). After H_2S release ceased, Fourier-transform infrared (FTIR) and powder XRD analyses of NaHS-Mg/Al(2/1) indicated that HS^- was partly replaced with CO_3^{2-}(Fig. 2G, 2H), supporting the air-stimulated anion-exchange mechanism. After H_2S release, only a trace amount of $S_2O_3^{2-}$ (1000−1200 cm^{-1}) was observed in the IR spectrum of NaHS-Mg/Al(2/1). In contrast, NaHS-Mg/Al(3/1), which ceased H_2S release within a few minutes (Fig. 2E), showed an intense IR signal from $S_2O_3^{2-}$ due to HS^- oxidation (Fig. S3).[24] Thus, HS^- tolerance against aerial oxidation is a crucial factor for long-term release of H_2S.

The amount of NaHS·nH$_2$O used in the synthesis of NaHS-Mg/Al(2/1)-type LDH was varied to find the optimum condition for obtaining the largest H_2S release (Fig. 2I). The concentration of the released H_2S increased with an increase in the amount of NaHS·nH$_2$O from 0.98 mg to 18.3 mg for 40 mg Cl^--type LDH, and the gross release reached maximum at 36.6 mg NaHS·nH$_2$O (=2.6 equivalent in mole for Cl^-). However, further addition of NaHS·nH$_2$O would reduce the gross release of H_2S, presumably due to increased basicity (i.e., OH^-) and impurities involved in the reaction solution.

Assuming that the chemical composition of NaHS-Mg/Al(2/1) with a maximum gross release is $Mg_2Al(OH)_6(HS^-)\cdot 2H_2O$ (Mw = 246.8 g/mol), 20 mg of the product involves 81 μmol of HS^-, which corresponds to a release of 76 ppm H_2S for 240 min (under 100 mL/min). The actual amount of H_2S released from NaHS-Mg/Al(2/1) was about half the expected value (Fig. 2I), which is attributable to an incomplete anion exchange from Cl^- to HS^- (see Section S7 in SI for discussion on chemical formula of NaHS-Mg/Al(2/1)).

It is widely known that NaHS and Na_2S also release odor characteristic to H_2S. However, these salts are highly deliquescent and strongly basic (pH ≥ 12). In contrast, NaHS-Mg/Al(2/1) is non-deliquescent, insoluble in water, and nearly neutral (pH ≈ 8), even when wet with water (Fig. S4). Moreover, Mg/Al-type LDH, known as hydrotalcite, is toxic-heavy-metal-free, biocompatible, and

practically utilized as an antacid drug.[25] These features of LDHs are advantageous for medical applications.

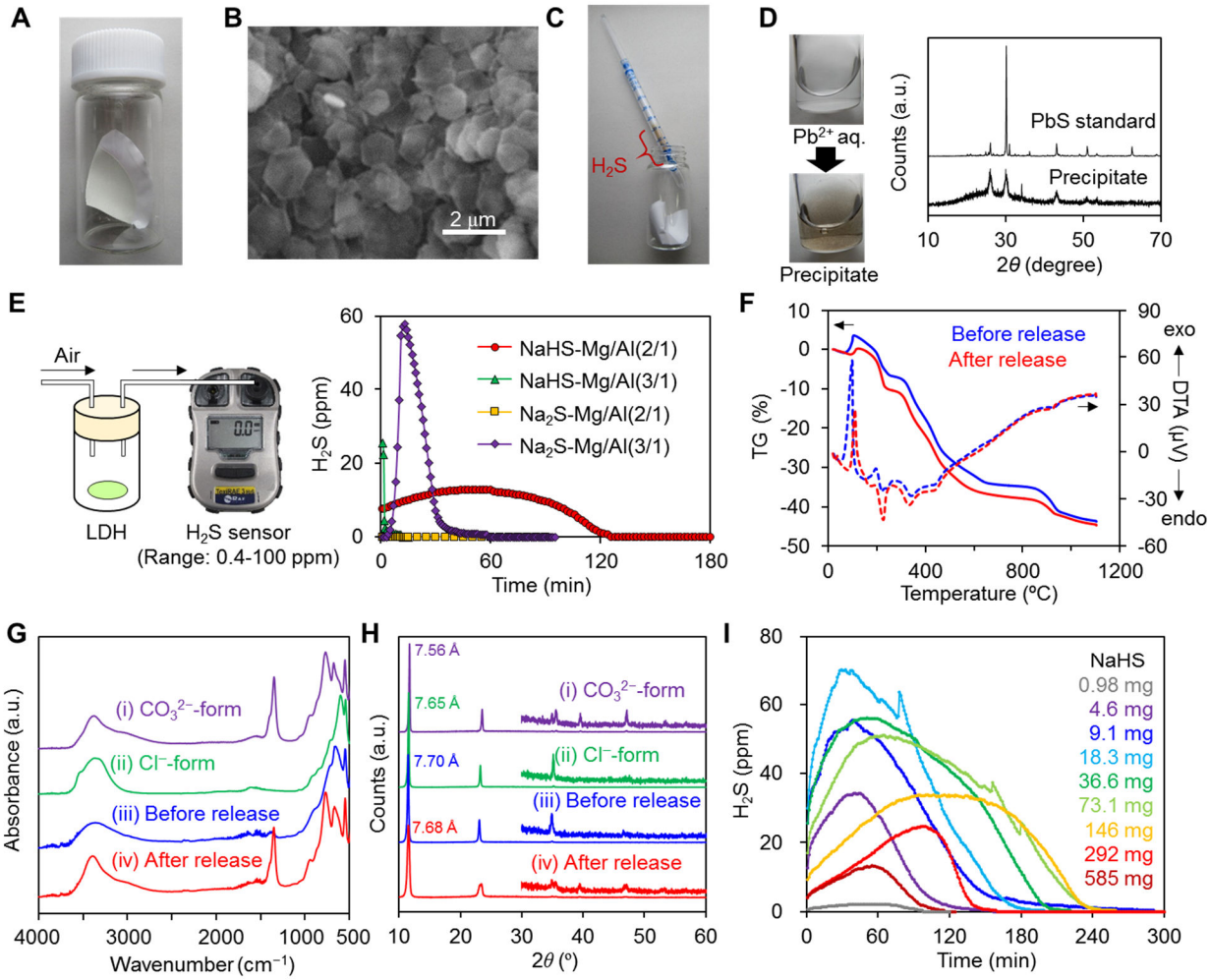

Fig. 2. Characterization of H_2S-releasing LDHs. (**A**) Photograph of NaHS-Mg/Al(2/1) embedded on membrane filter (stored in the glass vial purged with dry N_2). (**B**) SEM image of NaHS-Mg/Al(2/1) after H_2S release. (**C**) H_2S release from NaHS-Mg/Al(2/1) confirmed by detector tube. (**D**) Powder XRD pattern of black precipitate obtained by reaction of aqueous Pb^{2+} with released gas. (**E**) Continuous monitoring of H_2S released from LDHs under standard flow condition; 0.020 mmol of LDHs (5.0 mg of Mg/Al(2/1) and 6.25 mg of Mg/Al(3/1)) are tested. TG-DTA profiles (**F**), IR spectra (**G**), and powder XRD patterns (**H**) of NaHS-Mg/Al(2/1) before and after H_2S release. For comparison, IR and XRD data of starting materials are also shown. (**I**) Optimizing amount of NaHS·$n$$H_2O$ used in preparing NaHS-Mg/Al(2/1) from 40 mg of Cl^--type LDH; 20 mg of LDH was tested under standard flow condition.

Controlled release of H_2S from LDHs.

To reduce the interaction between NaHS-Mg/Al(2/1) and air for more steady and longer H_2S release, assembled materials with LDHs wrapped with porous tapes were prepared. About 1.1 mg of NaHS-

Mg/Al(2/1), which was synthesized under the optimum conditions using 40 mg LDH and 36.6 mg $NaHS{\cdot}nH_2O$ (Fig. 2I), was sandwiched between the membrane filters and further between the porous tapes (Fig. 3A, see Fig. S5 for details). As a result, the H_2S release profile was significantly improved compared to that of the bare (i.e., noncovered) material (Fig. 3B). Additionally, this patch-like assembly was effective in holding LDH powder.

The H_2S release profiles of the patch-like assembly were investigated under various conditions to probe the mechanisms and controllability of H_2S release. The H_2S concentration was almost proportional to the number of patch (Fig. 3B), which indicates ease of control of the gas concentration. The flow rate also affects the measured concentration: the H_2S concentration was inversely proportional to the flow rate of air (Fig. 3C). This means that the quantity of H_2S released from LDHs was almost constant. H_2S release was observed under a wide humidity range in air (10−87%RH), but the concentration reduced under fully dry air (Fig. 3D). H_2S release was not observed under dry N_2 and O_2 (Fig. 3E), but addition of humidity to N_2 induced H_2S release (Fig. 3F). As the pK_a values of H_2O (=7.0) and H_2S (=6.9) were close to each other, H_2O could be exchanged with interlayer HS^- through equilibrium (i.e., $[HS^-]_{LDH} + H_2O \rightarrow H_2S\uparrow + [OH^-]_{LDH}$). Addition of CO_2 into dry N_2 also caused H_2S release (Fig. 3G). In this process, the proton source must be interlayer H_2O, and the overall reaction is expressed as $2[HS^-]_{LDH} + CO_2 + [H_2O]_{LDH} \rightarrow 2H_2S\uparrow + [CO_3^{2-}]_{LDH}$. The activity of H_2S release was gradually quenched when exposed to dry O_2 beforehand, which is attributable to HS^- oxidation (Fig. S6). The H_2S concentration was slightly increased when heated to 36 °C (Fig. 3H), presumably due to accelerated diffusion of gas molecules and anions within the interlayer. LDHs preserved in a sealed pack for six months demonstrated a rather flat and elongated H_2S release (Fig. 3I). Mechanism of the aging effect could be homogenized distribution of HS^- within the interlayer. In fact, the aging effect can be accelerated by thermal treatment (e.g., 60 °C for several days) (Fig. S7).

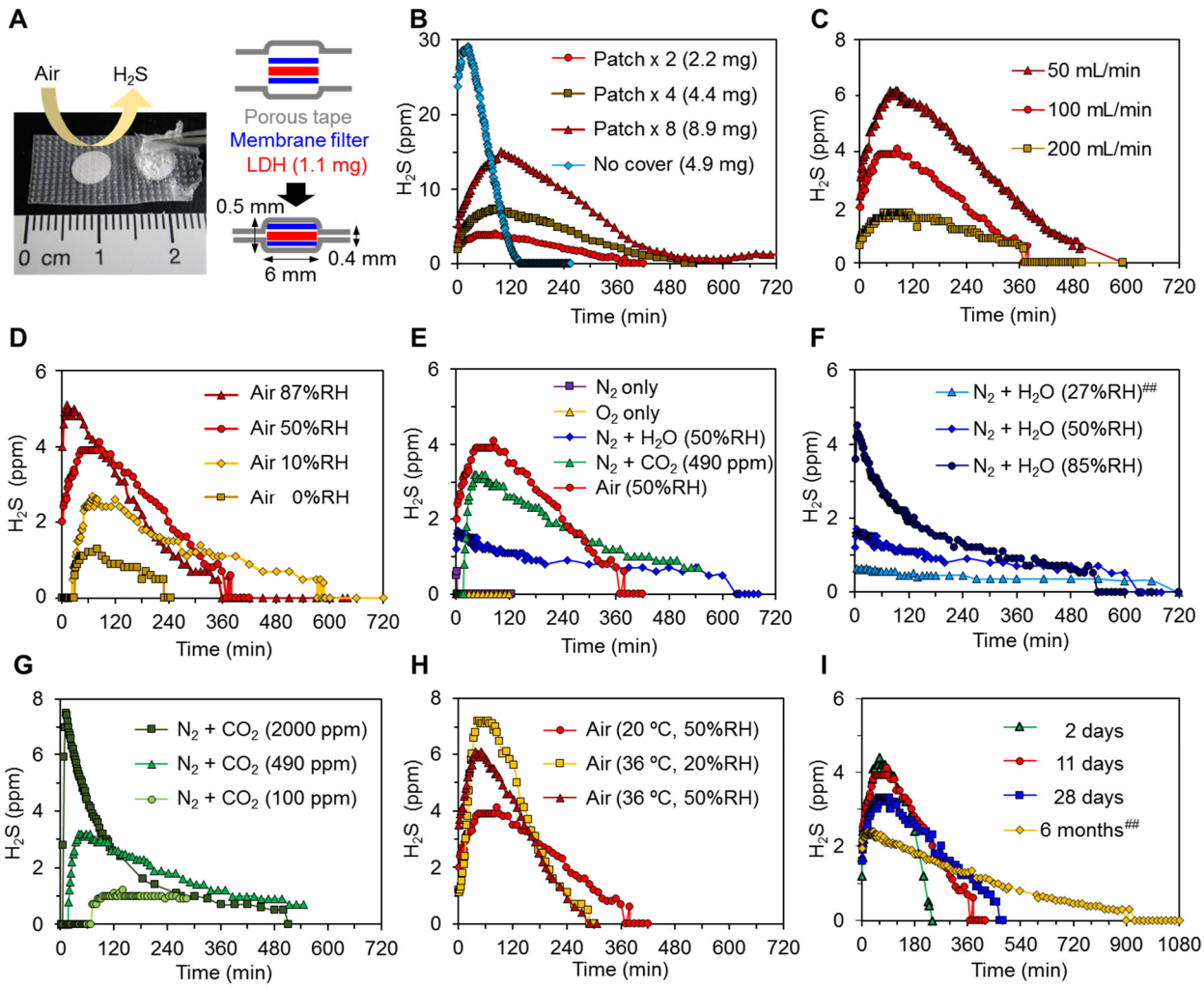

Fig. 3. H_2S release profiles from NaHS-Mg/Al(2/1) sandwiched between porous tapes.[#] (**A**) Photograph and illustration of H_2S release patches. One patch contains 1.1 mg of LDH. (**B**–**I**) Influences of various factor for H_2S release profiles; (**B**) patch numbers (release from noncovered sample is also shown for comparison), (**C**) flow rate of air, (**D**) humidity in air, (**E**) type of carrier gases, (**F**) humidity in N_2, (**G**) CO_2 concentration in dry N_2, (**H**) effect of temperature and humidity, and (**I**) aging effect. [#]Unless noted, H_2S release from two patches was tested under the standard flow condition. [##]Release from four patches was halved. See Schemes S1 and S2 for experimental set-up.

Controlled release of NO from LDHs.

LDHs involving NO_2^- were synthesized from Cl^--type LDHs (Mg:Al = 2:1 or 3:1) and $NaNO_2$, yielding $NaNO_2$-Mg/Al(2/1) and $NaNO_2$-Mg/Al(3/1) (183 mg $NaNO_2$ used for 40 mg LDHs, see SI for optimization of mixing ratio and discussion on chemical formula of the product). Release of HNO_2 from $NaNO_2$-Mg/Al(3/1) under air is suggested by visible color change of Griess reagent, which is a NO_2^- indicator[26] (Fig. 4A). The detector tube for NO + NO_2 demonstrates a positive response (0.7 ppm) for gases released from 100 mg $NaNO_2$-Mg/Al(3/1) under air (Fig. 4B-i). The concentration of nitrogenous gases released from LDHs was 2−3 orders of magnitude lower than that

of H_2S, probably because H_2CO_3 formed by CO_2 and water can afford fewer protons to NO_2^- than that to HS^- due to lower pK_a of HNO_2 (=~3.0).[27] On the other hand, release of nitrogenous gases was much longer, and continued for at least one day, maintaining similar concentration. Note that the detector tube for NO + NO_2 ("Tube-A") was equipped with the strong oxidant (Cr^{6+} + H_2SO_4) part at the entry for conversion of NO to NO_2, and its response should also involve the contribution of HNO_2. Thus, the total concentration, NO + NO_2 + HNO_2, was 0.7 ppm. Besides, NO_2 measured by another type of detector tube without the oxidant part ("Tube-B") was 0.2 ppm. NO was measured by combining two detector tubes, as follows. First, NO_2 and HNO_2 were removed by detector tube "B" for NO_2, which contains *o*-tolidine (aromatic amine) as an indicator. Here, acidic HNO_2 was removed by passing through this tube, but did not change color of the tube. In fact, after this treatment, the released gas did not change color of the Griess reagent, indicating complete removal of HNO_2 together with NO_2. Then, NO was determined as 0.2 ppm by the next detector tube, "A" for NO + NO_2. Thus, HNO_2 was estimated to be 0.3 ppm by subtracting 0.2 ppm of NO_2 and 0.2 ppm of NO from the total 0.7 ppm. The release of equal amounts (0.2 ppm) of NO and NO_2 indicates that these gases are derived from the disproportionation of HNO_2 (eq. 3 in Fig. 1C). Release of nitrogenous gases (NO + NO_2 + HNO_2) under air flow (100 mL/min) increased with humidity (0.5 ppm at 1.8%RH, 0.7 ppm at 35%RH, 1.1 ppm at 82%RH, and 1.6 ppm at 90%RH).

Compared to $NaNO_2$-Mg/Al(3/1), release of nitrogenous gases from $NaNO_2$-Mg/Al(2/1) was considerably small in air (~0.1 ppm or less) in the initial 2 h, while that of gases was gradually increased to ~1.5 ppm when the sample was further left in air. This delayed release profile resembles the case of NaHS-Mg/Al(2/1), where the anion-exchange reaction was regulated due to the narrow interlayer space.

Exhaled breath (4.0% CO_2, nearly saturated humidity, 100 mL/min) was applied to 100 mg $NaNO_2$-Mg/Al(3/1) for promoting protonation of interlayer NO_2^- (eq. 2 in Fig. 1B), and NO, NO_2, and HNO_2 measured by detector tubes were 1.0, 1.1, and 5.9 ppm, respectively (Fig. 4B-ii). HNO_2 can be reduced to NO using Fe^{2+} (eq. 4 in Fig. 1C),[19] and insertion of the $FeSO_4 \cdot 7H_2O$ column into the flow line successfully increased NO concentration to 6.6 ppm (Fig. 4B-iii). NO_2 was decreased to 0.55 ppm, presumably due to partial reduction to NO and/or adsorption on $FeSO_4 \cdot 7H_2O$. The total amount of nitrogenous gases (NO + NO_2 + HNO_2) was ~7.0 ppm, which means that the unreacted HNO_2 was negligible. The remaining NO_2 could be removed down to 0.02 ppm (only twice of the atmospheric level) using $Mg(OH)_2$, a selective adsorbent for acidic gases (Fig. 4B-iv).[28,29]

Release of NO from $NaNO_2$-Mg/Al(3/1) under exhaled breath continued over two weeks, as monitored by an electrochemical NO sensor, and its half-life of release was ~six days (Fig. 4C). The NO concentration did not increase in proportion to the quantity of materials (block connection in Fig. 4D-i). On the other hand, when $NaNO_2$-Mg/Al(3/1) and $FeSO_4 \cdot 7H_2O$ were alternatively connected (Fig. 4D-ii), the NO concentration could be increased in proportion to the quantity of the materials. This is because HNO_2 generation reached saturation under chemical equilibrium (eq. 2 in Fig. 1B) in

case of block connection, while HNO_2 was converted to neutral NO in each step without disturbing HNO_2 generation in the next step in case of the alternative connection.

The IR spectra of the as-prepared $NaNO_2$-Mg/Al(3/1) showed an intense absorption band of NO_2^- at 1227 cm^{-1} (Fig. S8). After the LDH was exposed to exhaled breath for two weeks, the NO_2^- signal was reduced, and concurrently, the CO_3^{2-} signal at 1360 cm^{-1} increased. This result indicates the dominant role of the CO_2-triggered anion-exchange reaction for HNO_2 release. XRD analyses also supported these results (Fig. S8).

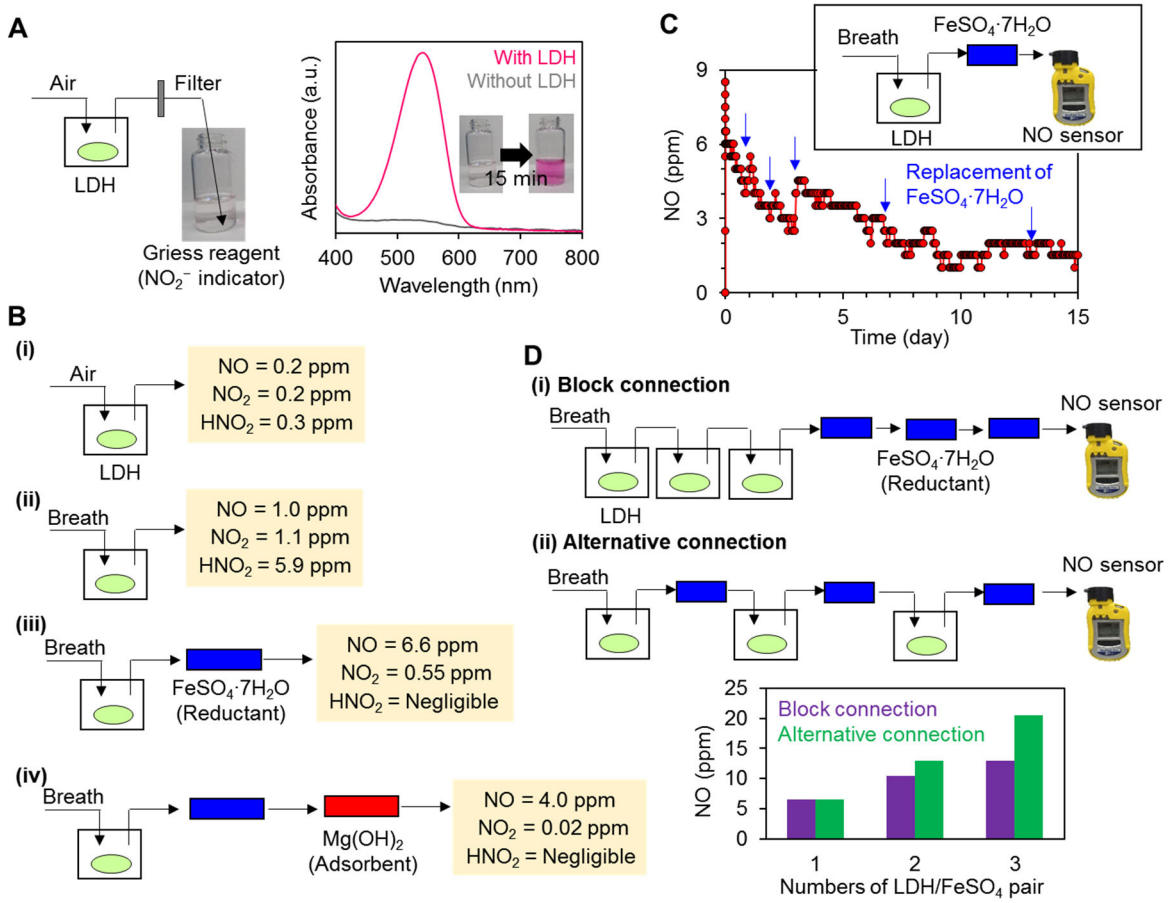

Fig. 4. Release of HNO_2 and conversion to NO. (**A**) Color change of Griess reagent showing the presence of HNO_2. (**B**) Concentrations of NO, NO_2, and HNO_2 released from 100 mg $NaNO_2$-Mg/Al(3/1) (determined by detector tube). See Scheme S3 for experimental details. (i) 100 mL/min air (20 °C, 35%RH) was applied. (ii-iv) 100 mL/min exhaled breath was applied. Released gases were passed through $FeSO_4{\cdot}7H_2O$ and $Mg(OH)_2$ loaded in the glass tube. (**C**) NO release profile from 100 mg $NaNO_2$-Mg/Al(3/1) under exhaled-breath flow (50 mL/min). $FeSO_4{\cdot}7H_2O$ was occasionally replaced with new ones (indicated by blue arrow). See Scheme S4 for experimental details. (**D**) Tandemly connected $NaNO_2$-Mg/Al(3/1) and $FeSO_4{\cdot}7H_2O$ (in block or alternative manner) for accumulating the concentration of NO under exhaled-breath flow (50 mL/min). Each vial contains 100 mg $NaNO_2$-Mg/Al(3/1). The NO concentration is monitored after stabilization for 15 min.

Battery-free respirator for inhaled-NO.

The potential utility of the air-stimulated gas release system was demonstrated by creating a portable and battery-free respirator that can supply therapeutically useful quantity of NO into inhaled air. The typical concentration of NO used for treatment of respiratory distress is 5−20 ppm,[10−14] and the respiratory volume of newborns and infants is ~0.5−2.5 L/min. Although the NO-release systems described in Fig. 4B−D, which are based on spatially isolated LDH and a reducing agent, provided NO over a week, limited quantity of NO (~1 ppm NO, 100 mL/min) could be obtained from 100 mg $NaNO_2$-Mg/Al(3/1) under air. Thus, it will require gram scale of materials to satisfy the criteria (5−20 ppm, 0.5−2.5 L/min) of inhaled-NO. In contrast, the results of Fig. 4D suggest that a spontaneous conversion of HNO_2 into NO is effective for NO accumulation (as a result of forwarding eq. 2 in Fig. 1B). Thus, we attempted to mix $NaNO_2$-Mg/Al(3/1) (100 mg) and $FeSO_4 \cdot 7H_2O$ (1.0 g) in powder form, and found that injection of wet air (100 mL/min) to the mixture led to release of highly concentrated NO (up to 650 ppm) **[CAUTION!!]**. After dilution with ambient air (4.0 L/min), 5−16 ppm NO was obtained for about 1 h (Fig. 5A). The use of $Mg(OH)_2$ effectively reduced the concentration of contaminated NO_2 to 0.03−0.075 ppm, which is much lower than the permissible limit of concentration determined by the U.S. Environmental Protection Agency (=1 ppm).[30]

The RH required to initiate NO release from the mixture was more than 60% (Fig. S9A), and the NO concentration could be adjusted by manipulating the RH (Fig. S9B). Moreover, we found that wet N_2 is also applicable (Fig. S9C). NO release under wet N_2 indicates that it is not governed by CO_2-triggered anion exchange, and a plausible mechanism is that the direct anion exchange between NO_2^- and SO_4^{2-} occurred in the mixed solids in a similar way as that reported for the anion exchange of LDHs in KBr powder[31] (Fig. S10A). Accordingly, self-reactive $Fe(NO_2)_2$ was formed outside LDHs, and then, NO_2^- was reduced to NO by Fe^{2+}. This hypothesis is supported by powder XRD patterns of post-release mixtures of $NaNO_2$-Mg/Al(3/1) and $FeSO_4 \cdot 7H_2O$, showing typical XRD patterns of SO_4^{2-}-type LDH (Fig. S10B).[32]

As shown in Fig. 5A, the concentration of NO release can be controlled by adjusting the amount of $NaNO_2$-Mg/Al(3/1). Moreover, the duration of NO release is elongated using $NaNO_2$-Mg/Al(2/1). After the release of NO, the mixture changed its color from aqua-blue to brown, implying the oxidation of Fe^{2+} to Fe^{3+} (Fig. 5B). The NO generation was further confirmed by other methods, including gas-phase IR spectroscopy and chemiluminescence (Figs. S11 and S12, Schemes S7 and S8). Moreover, NO_2^--incorporated LDHs were stable at RT as long as they were kept isolated from air (Fig. S9D).

Finally, we constructed a completely hand-operated (i.e., battery-free), disposable, and maintenance-free apparatus that can supply NO into the respirator (Fig. 5C). Wet air flow (~100 mL/min) was delivered to the mixture of $NaNO_2$-Mg/Al(3/1) and $FeSO_4 \cdot 7H_2O$ using a hand pump and humidifier (wet cotton). After passing through $Mg(OH)_2$, purified NO was mixed into the main air stream of the respirator. The NO concentration measured by the electrochemical sensor at the

respirator was consistent with the result shown in Fig. 5A. Besides the merits described above, following are the notable technical features of our gas delivery system: (i) low risk of overdose (as far as LDH amount is adequate) and (ii) visibility of gas generation (through Fe^{3+} formation). Additionally, if gas is released under N_2 flow, the obtained gas can be stored for a while without being oxidized.

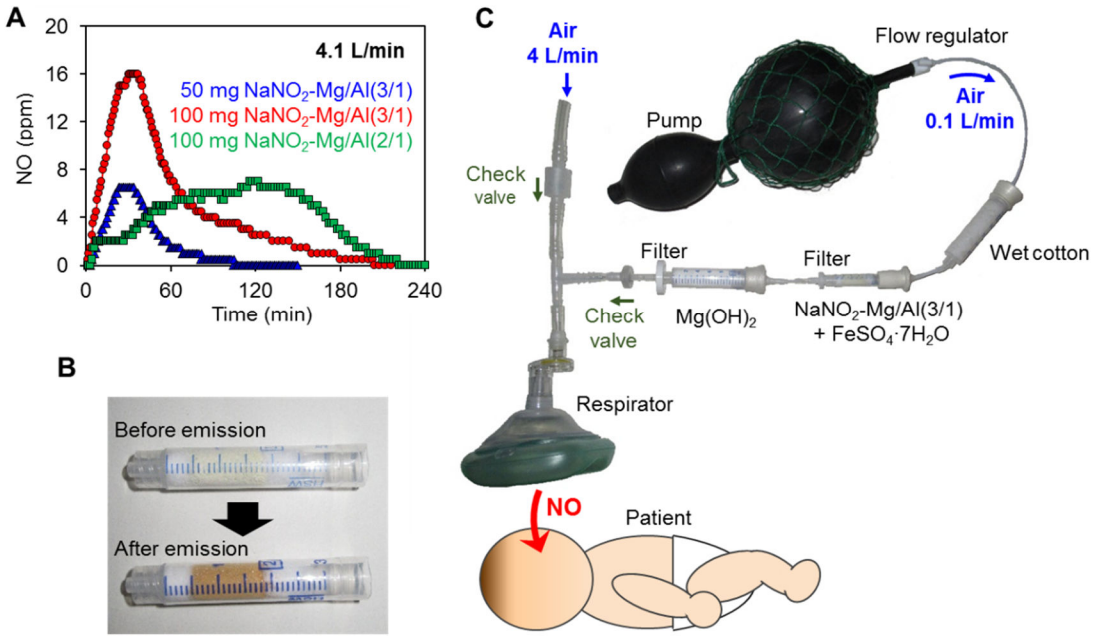

Fig. 5. Battery-free respirator for inhaled-NO. (**A**) Concentration of NO released from the mixture of NO_2^--incorporated LDH and 10 equivalent (in weight) of $FeSO_4 \cdot 7H_2O$ under 4.1 L/min air. See Scheme S5 for experimental set-up. (**B**) Photograph of $NaNO_2$-Mg/Al(3/1) and $FeSO_4 \cdot 7H_2O$ mixture before and after ending of NO release. (**C**) Prototype portable and battery-free respirator for inhaled-NO.

CONCLUSIONS

Solid materials that release ppm-level H_2S and NO in response to aerial components (H_2O and CO_2) are developed based on anion-exchange properties of LDHs at the solid−gas and solid−solid interfaces. The concentration and duration of gas release are controllable by adjusting various factors (composition of materials, diffusion of gas molecules and anions, and chemical equilibrium). Not only protic gases (i.e., H_2S and HNO_2) but also nonprotic gases (i.e., NO and NO_2) can be released by combining anion-exchange and redox reactions, which implies the applicability of our concept to broad ranges of gases. An air stimulus is safe, free of cost, and ubiquitous on earth; hence, LDH-based gas-release materials will expand opportunities of utilizing physiologically active (or other functional) gases in society, including application of inhaled-NO in developing countries and outside hospital.

Author Contributions.
S.I. and N.I. designed the research, performed experiments, and wrote the manuscript.

Acknowledgments.
This study was partly supported by a collaboration research grant from Sumitomo Seika Chemicals, Co. Ltd. and JSPS KAKENHI (Grant No. 18H02016). Mr. Daisuke Misho, Mr. Noriyuki Hayashizaka, Mr. Shunji Oyama, and Mr. Shigeki Sakaue (Sumitomo Seika Chemicals, Co. Ltd.) are acknowledged for fruitful discussion. Dr. Ya Xu (NIMS) is grateful for supporting NO analysis. Ms. Kumiko Hara and Ms. Reiko Takano are acknowledged for assisting research.

Competing interests.
NIMS and Sumitomo Seika Chemicals, Co. Ltd. filed a joint patent on H_2S-releasing materials, and NIMS solely filed a patent on NO_x-releasing materials and systems.

Data and material availability. All data needed to evaluate this study's conclusions are available in the main text and the supplementary materials.

SUPPLEMENTARY MATERIALS
Materials, methods, syntheses of LDHs, and monitoring and characterization of gases
Schemes S1 to S8
Figs. S1 to S15

REFERENCES
1. S. Chu, Y. Chi, N. Liu, The path towards sustainable energy. *Nat. Mater.* **16**, 16−22 (2017).
2. K. V. Kumar, K. Preuss, M.-M. Titirici, F. Rodríguez-Reinoso, Nanoporous materials for the onboard storage of natural gas. *Chem. Rev.* **117**, 1796−1825 (2017).
3. M. Götz *et al.*, Renewable power-to-gas: a technological and economic review. *Renew. Energy* **85**, 1371−1390 (2016).
4. L. Yu, P. Hu, Y. Chen, Gas-generating nanoplatforms: material chemistry, mulitifunctionality, and gas therapy. *Adv. Mater.* **30**, 1801964 (2018).
5. T. Yang, A. N. Zelikin, R. Chandrawati, Progress and promise of nitric oxide-releasing platforms. *Adv. Sci.* **5**, 1701043 (2018).
6. M. Kajimura, R. Fukuda, R. M. Bateman, T. Yamamoto, M. Suematsu, Interactions of multiple gas-transducing systems: hallmarks and uncertainties of CO, NO, and H_2S gas biology. *Antioxid. Redox Signaling* **13**, 157−192 (2010).
7. J. L. Wallace, Hydrogen sulfide-releasing anti-inflammatory drugs. *Trends Pharmacol. Sci.* **28**, 501–505 (2007).
8. C. Napoli, L. J. Ignarro, Nitric oxide-releasing drugs. *Annu. Rev. Pharmacol. Toxicol.* **43**, 97−123 (2003).
9. J. M. Carbajo, F. Maraver, Sulphurous mineral waters: new applications for health. *Evid.-Based Complementary Altern. Med.* **2017**, 8034084 (2017).

10. R. Rossanit, K. J. Falke, F. López, K. Slama, U. Pison, W. M. Zapol, Inhaled nitric oxide for the adult respiratory distress syndrome. *N. Eng. J. Med.* **328**, 399−405 (1993).
11. J. D. Roberts *et al*., Inhaled nitric oxide and persistent pulmonary hypertension of the newborn. *N. Eng. J. Med.* **336**, 605−610 (1997).
12. B. Yu, F. Ichinose, D. B. Bloch, W. M. Zapol, Inhaled nitric oxide. *Br. J. Pharmacol.* **176**, 246−255 (2019).
13. B. Yu, S. Muenster, A. H. Blaesi, D. B. Bloch, W. M. Zapol, Producing nitric oxide by pulsed electrical discharge in air for portable inhalation therapy. *Sci. Transl. Med.* **7**, 294ra107 (2015).
14. Y. Qin *et al.*, Portable nitric oxide (NO) generator based on electrochemical reduction of nitrite for potential applications in inhaled NO therapy and cardiopulmonary bypass surgery. *Mol. Pharmaceutics* **14**, 3762–3771 (2017).
15. Layered Double Hydroxide, ed. X. Duan and D. G. Evans, Springer, Heidelberg, 2006.
16. N. Iyi, Y. Ebina, T. Sasaki, Water-swellable MgAl-LDH (layered double hydroxide) hybrids: synthesis, characterization, and film preparation. *Langmuir* **24**, 5591−5598 (2008).
17. S. Ishihara *et al.*, Dynamic breathing of CO_2 by hydrotalcite. *J. Am. Chem. Soc.* **135**, 18040−18043 (2013).
18. P. Sahoo *et al.*, Rapid exchange between atmospheric CO_2 and carbonate anion intercalated within magnesium rich layered double hydroxide. *ACS Appl. Mater. Interfaces* **6**, 18352–18359 (2014).
19. Advanced Inorganic Chemistry, Fourth Edition. By F. A. Cotton, G. Wilkinson, John Wiley & Sons, Inc.: New York, 1980.
20. S. Ma *et al.*, Highly efficient iodine capture by layered double hydroxides intercalated with polysulfides. *Chem. Mater.* **26**, 7114−7123 (2014).
21. N. Iyi, T. Matsumoto, Y. Kaneko, K. Kitamura. A novel synthetic route to layered double hydroxides using hexamethylenetetramine. *Chem. Lett.* **33**, 1122−1123 (2004).
22. N. Iyi, H. Yamada, T. Sasaki. Deintercalation of carbonate ions from carbonate-type layered double hydroxides (LDHs) using acid-alcohol mixed solutions. *Applied Clay Sci.* **54**, 132−137 (2011).
23. M. Ogawa, F. Saito, Easily oxidizable polysulfide anion occluded in the interlayer space of Mg/Al layered double hydroxide. *Chem. Lett.* **33**, 1030−1031 (2004).
24. M.Sato, H. Kuwabara, S. Saito, Characterization of anion exchanged hydrotalcite and determination of the site of exchanged SO_4 group. *Clay Sci.* **8**, 309−317 (1992).
25. J.-H. Choy, S.-J. Choi, J.-M. Oh, T. Park, Clay minerals and layered double hydroxides for novel biological applications. *Appl. Clay Sci.* **36**, 122−132 (2007).
26. E. M. Hetrick, M. H. Schoenfisch, Analytical chemistry of nitric oxide. *Annu. Rev. Anal. Chem.* **2**, 409−433 (2009).
27. G. da Silva, E. M. Kennedy, B. Z. Dlugogorski, Ab initio procedure for aqueous-phase p*K*a calculation: the acidity of nitrous acid. *J. Phys. Chem. A* **110**, 11371−11376 (2006).
28. E. Sada, H. Kumazawa, M. A. Butt, Single and simultaneous absorptions of lean SO_2 and NO_2 into aqueous slurries of $Ca(OH)_2$ or $Mg(OH)_2$ particles. *J. Chem. Eng. Jpn.* **12**, 111−117 (1979).
29. F. Rezaei, A. A. Rownaghi, S. Monjezi, R. P. Lively, C. W. Jones, SO_x/NO_x removal from fuel gas streams by solid adsorbents: a review of current challenges and future directions. *Energy Fuels* **29**, 5467−5486 (2015).
30. 1988 OSHA PEL Project Documentation (Centers for Disease Control and Prevention, Atlanta, GA, 1988).
31. N. Iyi, F. Geng, T. Sasaki, Effect of KBr on the FTIR spectra of NO_3^-LDHs (layered double hydroxides). *Chem. Lett.* **38**, 808−809 (2009).

32. N. Iyi, K. Fujii, K. Okamoto, T. Sasaki, Factors influencing the hydration of layered double hydroxides (LDHs) and the appearance of an intermediate second staging phase. *Appl. Clay Sci.* **35**, 218−227 (2007).

SUPPLEMENTARY MATERIALS

Controlled Release of H_2S and NO through Air-Stimulated Anion Exchange

Shinsuke Ishihara* and Nobuo Iyi*

International Center for Materials Nanoarchitectonics (WPI-MANA), National Institute for Materials Science (NIMS), 1-1 Namiki, Tsukuba, Ibaraki 305-0044, Japan

*Corresponding author.
Email: ISHIHARA.Shinsuke@nims.go.jp, IYI.Nobuo@nims.go.jp

Table of Contents

S1. Materials.

$NaHS{\cdot}nH_2O$ (65%), $Na_2S{\cdot}9H_2O$, and $NaNO_2$ were obtained from Wako Pure Chemical Industries, Ltd. Granular $FeSO_4{\cdot}7H_2O$ (Fujifilm Wako Pure Chemical Corp.) was ground on a mortar to prepare powdered samples. $Mg(OH)_2$, 0.1 mol/L HCl in ethanol, and 3% HCl in ethanol were purchased from Kanto Chemical Co., Inc. Methanol, PbS, and $Pb(CH_3COO)_2{\cdot}3H_2O$ were obtained from Nakalai Tesque, Inc. Griess reagent (Sigma-Aldrich) was used as received. The gas cylinder (compressed dry air, CO_2, 25.1 ppm H_2S in N_2, 24.9 ppm NO in N_2) was obtained from Suzuki Shokan Co., Ltd. Water was deionized using PURELAB Option-S7/15 (ELGA), and then degassed by boiling for 15 min under N_2 bubbling (0.1−0.3 L/min), followed by cooling down to RT under the same N_2-bubbling condition. Degassed deionized water was stored in a sealed glass bottle and used for synthesis of LDHs. $Mg_3Al(OH)_8(CO_3^{2-})_{0.5}{\cdot}2H_2O$ was purchased from Kyowa Kagaku Kogyo Co., Ltd. $Mg_2Al(OH)_6(CO_3^{2-})_{0.5}{\cdot}2H_2O$ was prepared by a hydrothermal reaction according to literature procedure.[21] $Mg_3Al(OH)_8(Cl^-){\cdot}2H_2O$ and $Mg_2Al(OH)_6(Cl^-){\cdot}2H_2O$ were prepared by an anion-exchange reaction according to a previously reported procedure.[18,22] A porous tape (KEEP PORE™, 25 mm × 8 m) was obtained from Nichiban Co., Ltd. A hydrophilic PTFE membrane filter (Omnipore™ membrane filter JGWP04700, pore size = 0.2 μm, diameter = 47 mm) obtained from Merck Millipore, Ltd., was utilized for filtration of LDH products. A small syringe filter (Cosmonice filter S, Pore size = 0.45 μm, Filter diameter = 13 mm) was purchased from Nakalai Tesque, Inc. A large syringe filter (PFSF-2545PT, pore size = 0.45 μm, filter diameter = 25 mm) was purchased from AS ONE Corporation.

S2. General methods.

FT-IR spectra of the powdered sample were measured by IR Affinity-1 (Shimadzu) in ATR mode, as well as by Spectrum One FT-IR apparatus with ATR attachment (Perkin-Elmer). Powder XRD was measured by RINT2200V (Rigaku Co., Ltd.) with CuK_{α} at a scan rate of 2 ^{o}/min under dry N_2-flow. TG-DTA was measured by ThermoPlus TG8120 (Rigaku Co., Ltd.) at a heating rate of 10 °C/min under air flow (20 mL/min). Approximately 10 mg of LDH in a Pt pan was measured, and α-Al_2O_3 was used as a standard. The SEM image was monitored by S-4800 (Hitachi) at 10 kV. The energy-dispersive X-ray spectrometry (EDS) spectrum was measured by SEM-EDS apparatus (JEOL, JSM6010LA) at an acceleration voltage of 10−15 kV. Powdery LDH on the carbon tape was monitored without coating of conductive layers. The electric absorption spectrum was measured using UV-3600 (Shimadzu) at RT. CO_2 was monitored by TESTO 535 (TESTO) within a detection range of 0−9999 ppm (resolution = 1 ppm). O_2 was monitored by a digital sensor (Oxy-M and Oxy-1S-M, ICHINEN JIKCO., Ltd.). RH was monitored by HMI-41 (VAISALA). The flow rate was monitored by a float-ball-type flow meter (KOFLOCK) or a digital flow meter (7000 Flowmeter, Ellutia). A digital camera in the time-lapse mode (EX-ZR1800, CASHIO) was utilized for recording values of gas sensors every 1−5 min. All detector tubes (No.4L for H_2S, No.5Lb for SO_2, No.9P for NO_2, No.11L for $NO+NO_2$, and No.10 for separate quantification of NO and NO_2) were purchased from GASTEC. Sampling of gases using the detector tube was performed with a handy pump (GV-100S, GASTEC) or a battery-powered pump (GSP-300FT-2 or GSP-400FT, GASTEC). An electric oven (IW-300S or AVO-250NB, ETTAS) was used to heat samples at constant temperature.

S3. Syntheses of LDHs.

Table S1. Syntheses of LDH-based H_2S-releasing materials.

Product name	LDH precursor (mg, mmol)	Sulfide reagent (mg, mmol)	Peak of H_2S release#
NaHS-Mg/Al(2/1)	$Mg_2Al(OH)_6(Cl^-)\cdot 2H_2O$ (40 mg, 0.16 mmol)	$NaHS\cdot nH_2O$ (141 mg, 1.63 mmol)	12.6 ppm at 52 min
NaHS-Mg/Al(3/1)	$Mg_3Al(OH)_8(Cl^-)\cdot 2H_2O$ (50 mg, 0.16 mmol)	$NaHS\cdot nH_2O$ (141 mg, 1.63 mmol)	25.4 ppm at 1 min
Na_2S-Mg/Al(2/1)	$Mg_2Al(OH)_6(Cl^-)\cdot 2H_2O$ (40 mg, 0.16mmol)	$Na_2S\cdot 9H_2O$ (393 mg, 1.63 mmol)	No emission
Na_2S-Mg/Al(3/1)	$Mg_3Al(OH)_8(Cl^-)\cdot 2H_2O$ (50 mg, 0.16 mmol)	$Na_2S\cdot 9H_2O$ (393 mg, 1.63 mmol)	57.8 ppm at 13 min

#Data from Fig. 2E.

S3.1. Syntheses of NaHS-Mg/Al(2/1) and NaHS-Mg/Al(3/1)

All experiments (except for sonication) were performed under dry N_2 using a globe box. To 40 mg of $Mg_2Al(OH)_6(Cl^-)\cdot 2H_2O$ or 50 mg of $Mg_3Al(OH)_8(Cl^-)\cdot 2H_2O$ in a screw-cap glass vial (50 mL), degassed deionized water (22.8 mL) was added, and then, 7.2 mL of $NaHS\cdot nH_2O$ dissolved in degassed deionized water (19.5 mg/mL). After closing the screw cap tightly, the glass bottle (taken out from globe box) was soaked in an ultrasonication bath for dispersion of LDH particles (for ~30 s). The glass bottle was stored at RT under N_2 for 2 days. The suspension was filtered on the PTFE membrane filter (Omnipore™, pore size = 0.2 μm) and washed with degassed deionized water (2 mL × 5 times). The membrane filter with the sample was cut to a desired size (e.g., semicircle and quadrant), and dried in vacuum for 3 h. The solid sample on the membrane filter was kept in a screw-cap glass vial (13.5 mL), which, if necessary, was stored in a gas barrier bag (Lamizip® AL-D, Seisannipponsha, Ltd.). Yield: quantitative. When changing the amount of $NaHS\cdot nH_2O$, the mixing ratio of degassed deionized water and aqueous solution of $NaHS\cdot nH_2O$ (19.5 mg/mL) was varied for maintaining the total volume of the solution at 30 mL.

S3.2. Syntheses of Na_2S-Mg/Al(2/1) and Na_2S-Mg/Al(3/1)

All experiments (except for sonication) were performed under dry N_2 using a globe box. To 40 mg of $Mg_2Al(OH)_6(Cl^-)\cdot 2H_2O$ or 50 mg of $Mg_3Al(OH)_8(Cl^-)\cdot 2H_2O$ in the screw-cap glass vial (50 mL), degassed deionized water (27.2 mL) was added, and then, 2.8 mL of $Na_2S\cdot 9H_2O$ dissolved in degassed deionized water (139.3 mg/mL). After closing the screw cap tightly, the glass bottle (taken out from globe box) was soaked in an ultrasonication bath for dispersion of LDH particles (for ~30 s). The glass bottle was stored at room temperature under N_2 for 2 days. The suspension was filtered on the PTFE membrane filter (Omnipore™, pore size = 0.2 μm) and washed with degassed

deionized water (2 mL × 5 times). The membrane filter with the sample was cut to the desired size (e.g., semicircle and quadrant), and dried in vacuum for 3 h. The solid sample on the membrane filter was kept in the screw-cap glass vial (13.5 mL), which if necessary, was stored in gas barrier bag (Lamizip® AL-D, Seisannipponsha, Ltd.). Yield: quantitative.

S3.3. Syntheses of NaHS-Mg/Al(2/1) in methanol

All experiments (except for sonication) were performed under dry N_2 using a globe box. To 20 mg of $Mg_2Al(OH)_6(Cl^-)\cdot 2H_2O$ in the screw-cap glass vial (40 mL), degassed methanol (20 mL) containing 7.25 mg of $NaHS\cdot nH_2O$ was added. Two batches were prepared. After closing the screw cap tightly, the glass bottle (taken out from the globe box) was soaked in an ultrasonication bath for dispersion of LDH particles until fully dispersed suspensions were formed. The two glass bottles were stored at RT under N_2 for 2 days. The suspension in one vessel was filtered on the PTFE membrane filter (Omnipore^{TM}, pore size = 0.2 μm) and washed with degassed methanol. Another suspension was filtered on the PTFE membrane filter (pore size = 0.2 μm) and washed with degassed deionized water of the same amount with MeOH. Each membrane filter was folded to a semicircle (with sample inside), and then cut into four fan-shaped isometric pieces. Each piece containing 5.0 mg NaHS-Mg/Al(2/1) was put into a glass vial, and dried in vacuum for 40 min. Each sample was kept in a screw-cap glass vial (13.5 mL). These samples were utilized only for discussing Fig. S15.

S3.4. Small-scale syntheses of $NaNO_2$-Mg/Al(2/1) and $NaNO_2$-Mg/Al(3/1) in globe box

All experiments (except for sonication) were performed under dry N_2 using a globe box. To 40 mg of $Mg_2Al(OH)_6(Cl^-)\cdot 2H_2O$ or $Mg_3Al(OH)_8(Cl^-)\cdot 2H_2O$ in a screw-cap glass vial (50 mL), degassed deionized water (28.2 mL) was added, and then, 1.8 mL of $NaNO_2$ dissolved in degassed deionized water (100 mg/mL). After closing the screw cap tightly, the glass bottle (taken out from the globe box) was soaked in an ultrasonication bath for dispersion of LDH particles (for ~30 s). The glass bottle was returned to the globe box and stored at RT under N_2 for 2 days. The suspension was filtered on the PTFE membrane filter (Omnipore^{TM}, pore size = 0.2 μm), and washed with degassed deionized water (2 mL × 5 times). The membrane filter with the sample was cut to the desired size (e.g., semicircle and quadrant), and dried in vacuum for 3 h. The white solid sample on the membrane filter was kept in a screw-cap glass vial (13.5 mL), which if necessary, was stored in a gas barrier bag (Lamizip® AL-D, Seisannipponsha, Ltd.). Yield: quantitative. When changing the amount of $NaNO_2$, the mixing ratio of degassed deionized water and aqueous solution of $NaNO_2$ (100 mg/mL) was varied for maintaining the total volume of the solution as 30 mL. The amount of $NaNO_2$ used in the synthesis of $NaNO_2$-Mg/Al(3/1) was optimized by comparing three conditions (36.5, 183, or 914 mg of $NaNO_2$ for 40 mg $Mg_3Al(OH)_8(Cl^-)\cdot 2H_2O$). $NaNO_2$-Mg/Al(3/1) prepared from 183 mg $NaNO_2$ demonstrated 0.5 ppm of NO + NO_2 + HNO_2 (tested by detector tube, GASTEC−11L) after exposure to air for 30 min. In contrast, $NaNO_2$-Mg/Al(3/1) prepared from 36.5 mg $NaNO_2$ and 914 mg $NaNO_2$ demonstrated 0.4 ppm and 0.25 ppm of NO + NO_2 + HNO_2,

respectively. Thus, 183 mg $NaNO_2$ (20.4 equivalent in mole for Cl^-) was found as the optimal mixing amount for 40 mg of $Mg_3Al(OH)_8(Cl^-)\cdot 2H_2O$. As NO release experiments require gram scale of NO_2^--incorporated LDHs in total, we chose $NaNO_2$-Mg/Al(3/1) for the main study. $Mg_3Al(OH)_8(CO_3^{2-})_{0.5}\cdot 2H_2O$ is commercially available on the kilogram scale, but $Mg_2Al(OH)_6(CO_3^{2-})_{0.5}\cdot 2H_2O$ must be synthesized by a hydrothermal reaction.

S3.5. Large-scale synthesis of $NaNO_2$-Mg/Al(3/1) without globe box

To 2.0 g of $Mg_3Al(OH)_8(Cl^-)\cdot 2H_2O$ in a round-bottom three-neck flask (500 mL), degassed deionized water (300 mL) was added after purging the flask with dry N_2. The flask was soaked in an ultrasonication bath for dispersion of LDH particles (for ~3 min). Then, 9.5 g of $NaNO_2$ dissolved in degassed deionized water (40 mL) was added to the solution using a needle syringe through a rubber septum. The suspension was stirred under N_2 for one day, and then, left standing without stirring for another day. The suspension was filtered on a PTFE membrane filter (Omnipore^{TM}, pore size = 0.2 μm) under N_2, washed with degassed deionized water (10 mL × 3 times) and methanol (10 mL × 1), and dried in vacuum at 40 °C for 5 h. The white solid sample on the membrane filter was kept in a screw-cap glass vial (13.5 mL). The sample was stable over months when kept in the screw-cap glass vial. Yield: 1.9 g. $NaNO_2$-Mg/Al(3/1) prepared in this method shows an identical IR spectrum to that of $NaNO_2$-Mg/Al(3/1) prepared in the globe box.

S4. Monitoring H_2S

S4.1. Precipitation of Pb^{2+}

We bubbled 38 mg of $Pb(CH_3COO)_2 \cdot 3H_2O$ dissolved in 10 mL distilled H_2O with H_2S released from four patches of NaHS-Mg/Al(2/1) (Fig. 3A) under ambient air flow (100 mL/min, 76%RH). After 1 h, the formed black precipitate was collected by centrifugation, followed by washing with water, diluted acetic acid (0.05 mL acetic acid in 20 mL H_2O), and methanol. The use of dilute acetic acid was effective in removing the white precipitate ($Pd(CO_3)$ and/or $Pd(OH)_2$) that appeared even when $Pb(CH_3COO)_2$ aqueous solution was bubbled with air. The black precipitate was dispersed in methanol, and the suspension was spread on a glass plate. After drying methanol, powder XRD was measured. PbS standard was also dispersed in methanol, and the suspension was spread on a glass plate. After drying methanol, powder XRD was measured.

S4.2. Detector tube

Detector tubes for H_2S (GASTEC−4L) and SO_2 (GASTEC−5Lb) were utilized for quantitative monitoring of the corresponding gases.

S4.3. Gas sensor

H_2S was monitored using an electrochemical sensor (ToxiRAE 3, RAE SYSTEMS) within a detection range of 0.4−100 ppm (resolution = 0.1 ppm). The H_2S electrochemical sensor was calibrated by standard gas (25.1 ppm H_2S in N_2). Compressed dry air (containing CO_2 and other minor components of atmospheric air) was supplied from the gas cylinder, and humidity was adjusted as shown in Scheme S1. Dry N_2 containing adjusted amount of CO_2 was delivered as shown in Scheme S2 using a Tedlar® bag and an electric pump (GSP-400FT, GASTEC). Unless noted, all gas release experiments were performed after aging the LDH samples attached on the membrane filter for about 1 week at RT (to reduce aging effect in sample-to-sample comparison). The volume of the glass vial used for LDH storage was 13.5 mL.

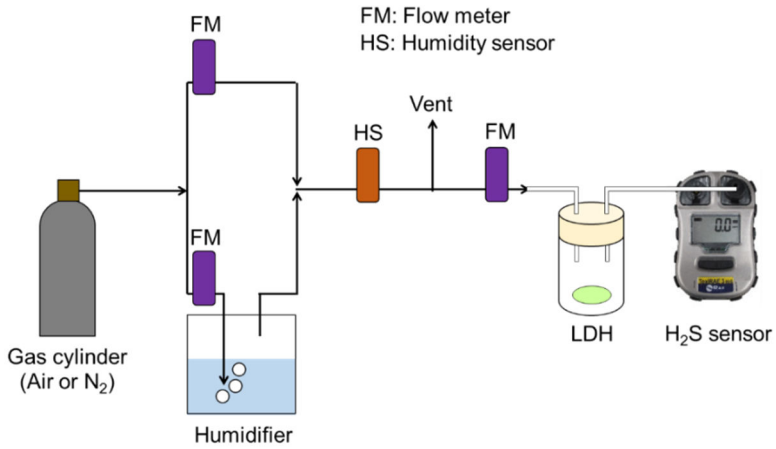

Scheme S1. Experimental set-up for delivering carrier gas with adjusted humidity and flow rate. When necessary, LDH in glass vial was warmed in an electric oven.

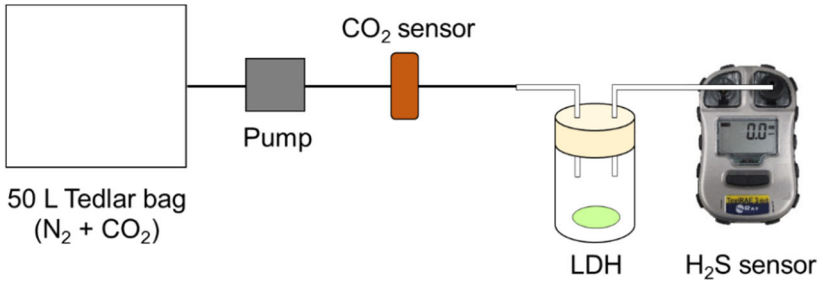

Scheme S2. Typical experimental set-up for delivering dry N_2 containing CO_2. This experiment was performed in a globe box (dry N_2 atmosphere) for avoiding contamination of trace humidity from air. For example, 100 ppm CO_2 in N_2 was prepared by adding 5 mL CO_2 into 50 L N_2 filled in the Tedlar® bag. The volume of the glass vial used for LDH storage was 13.5 mL.

S5. Monitoring NO_x

S5.1. Griess reagent

An aqueous solution of Griess reagent (NO^- indicator) was prepared by dissolving 1.0 g Griess reagent (Sigma-Aldrich) in 25 mL of distilled water. Then, 100 mL/min of ambient air (20 °C, 35%RH) was passed through the glass vial containing 100 mg $NaNO_2$-Mg/Al(3/1), followed by bubbling of the gas into the aqueous solution of the Griess reagent (3 mL). After 15 min bubbling, the absorption spectra of the solution were measured using a 1 cm quarts cell. Note that the Griess reagent also responds to NO_2 as NO_2 produces HNO_2 in water ($2NO_2 + H_2O \rightarrow HNO_3 + HNO_2$).

S5.2. Detector tube

NO, NO_2, and HNO_2 were monitored by combining several detector tubes. Humidity-controlled air or exhaled breath (involving 4.0% CO_2 and saturated humidity) was supplied by an electric pump to 100 mg $NaNO_2$-Mg/Al(3/1), as shown in Scheme S3. When necessary, granular $FeSO4 \cdot 7H_2O$ (~750 mg, 3 cm in length) and powdery $Mg(OH)_2$ (~250 mg, 3 cm in length) loaded in the glass tube were inserted into the flow line for converting HNO_2 to NO and removing NO_2, respectively. As the permissible humidity range of the detector tubes was 0−90%, the sampling gas was diluted with the same amount of dry air (i.e., RH was adjusted to ~50%RH upon monitoring with the detector tube). Therefore, the actual concentration of analyte gases was twice the value shown by the detector tubes. The NO_2 concentration was determined using GASTEC−9P, which is insensitive to HNO_2 and NO. The gas sampling rate was 100 mL/min. Concentration of NO + NO_2 + HNO_2 was determined using GASTEC−11L, which involved a strong oxidant (Cr^{3+} + H_2SO_4) at the entry for converting NO to NO_2. HNO_2 should be oxidized to NO_2 as well. Then, the resulting NO_2 was quantified by *o*-tolidine (aromatic amine), a NO_2 indicator. The standard sampling rate for GASTEC−11L was 50 mL/min, so that excess gas was vented outside using the check valve. The NO concentration was determined by combining two detector tubes, GASTEC−10 (for NO_2) and GASTEC−11L, as shown in Scheme S3. NO_2 and HNO_2 were removed by the first detector tube for NO_2 (GASTEC−10), which contains *o*-tolidine. NO could pass through this tube, and then was detected by the second detector tube (GASTEC−11L) after conversion to NO_2. The HNO_2 concentration was estimated by subtracting NO and NO_2 from NO + NO_2 + HNO_2.

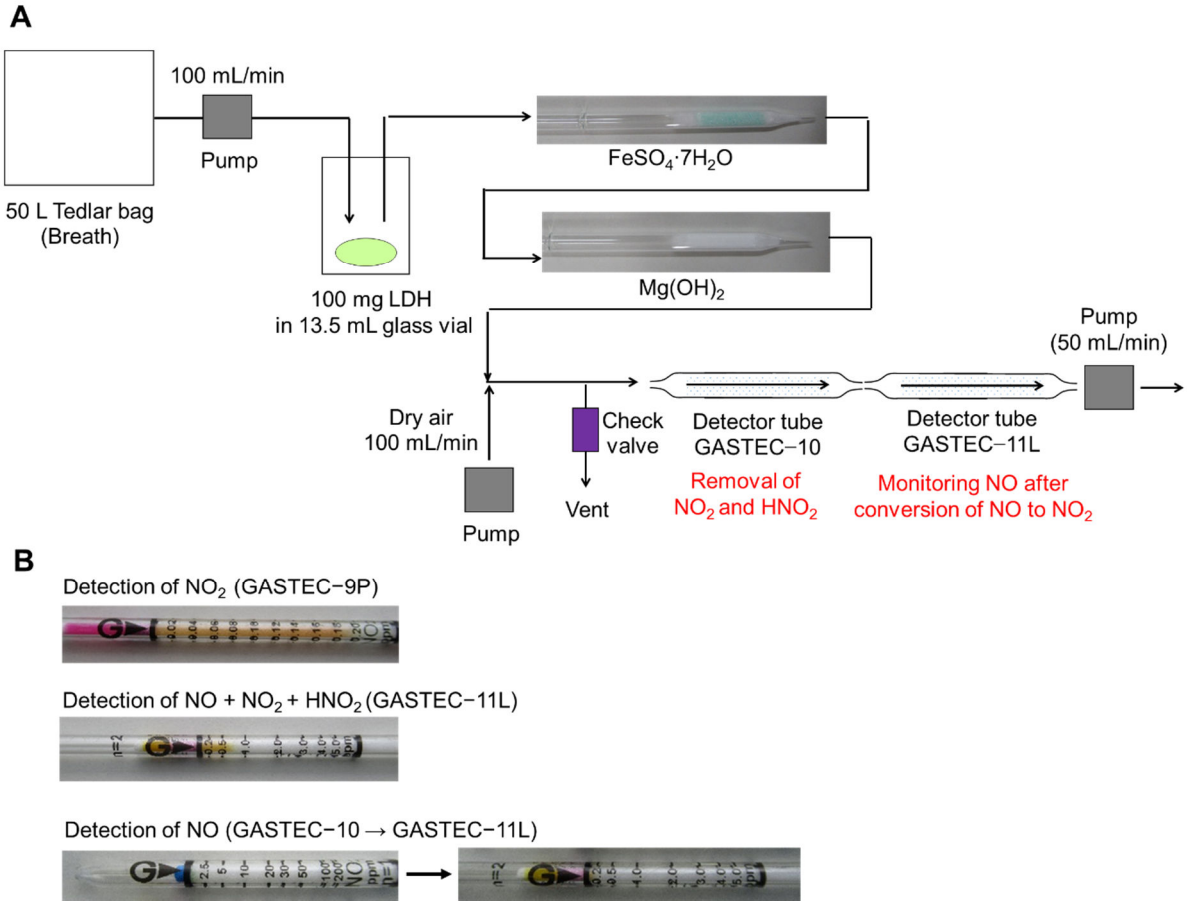

Scheme S3. (**A**) Typical experimental set-up for monitoring NO, NO_2, and HNO_2 by detector tube. The image specifically shows NO detection. (**B**) Typical images of detector tubes responding to nitrogenous gases.

S5.3. Gas sensor

NO was monitored by a digital sensor (ToxiRAE Pro, RAE SYSTEMS) within a detection range of 0.5−250 ppm (resolution = 0.5 ppm). The NO digital sensor was calibrated by standard gas (24.9 ppm NO in N_2). Exhaled breath (containing 4.0% CO_2 and saturated relative humidity) in a Tedlar® bag was delivered by an electrical pump, as shown in Scheme S4. HNO_2 was converted to NO using granular $FeSO_4{\cdot}7H_2O$ (~750 mg, 3 cm in length), and monitored by a NO sensor. $FeSO_4{\cdot}7H_2O$ was occasionally changed to new ones.

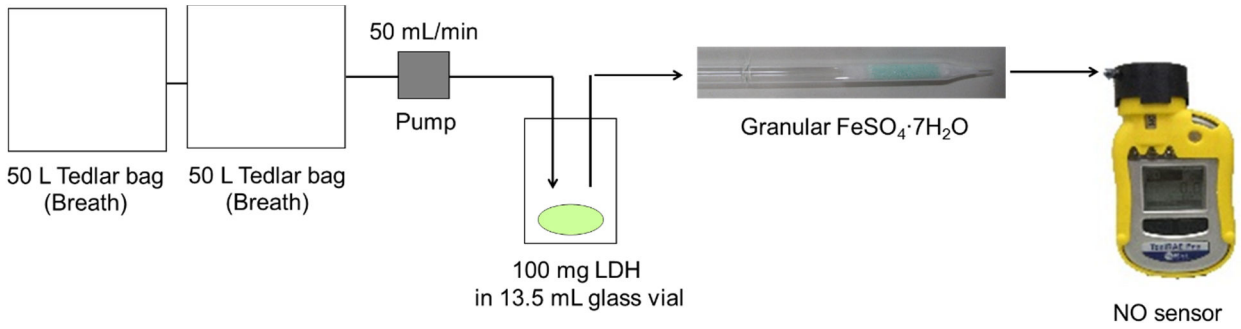

Scheme S4. Typical experimental set-up for monitoring NO by electrochemical sensor.

Release of NO from a mixture of 100 mg $NaNO_2$-Mg/Al(3/1) and 1.0 g $FeSO_4 \cdot 7H_2O$ was monitored as shown in Scheme S5. Humid air (100 mL/min) was delivered to the mixture, and then, contaminated NO_2 was removed by 4.0 g of $Mg(OH)_2$ loaded in a 12 mL plastic syringe. NO was diluted with 4.0 L/min air and monitored by an electrochemical sensor (ToxiRAE Pro, RAE SYSTEMS). The NO_2 concentration was occasionally monitored by a detector tube (GASTEC−9P).

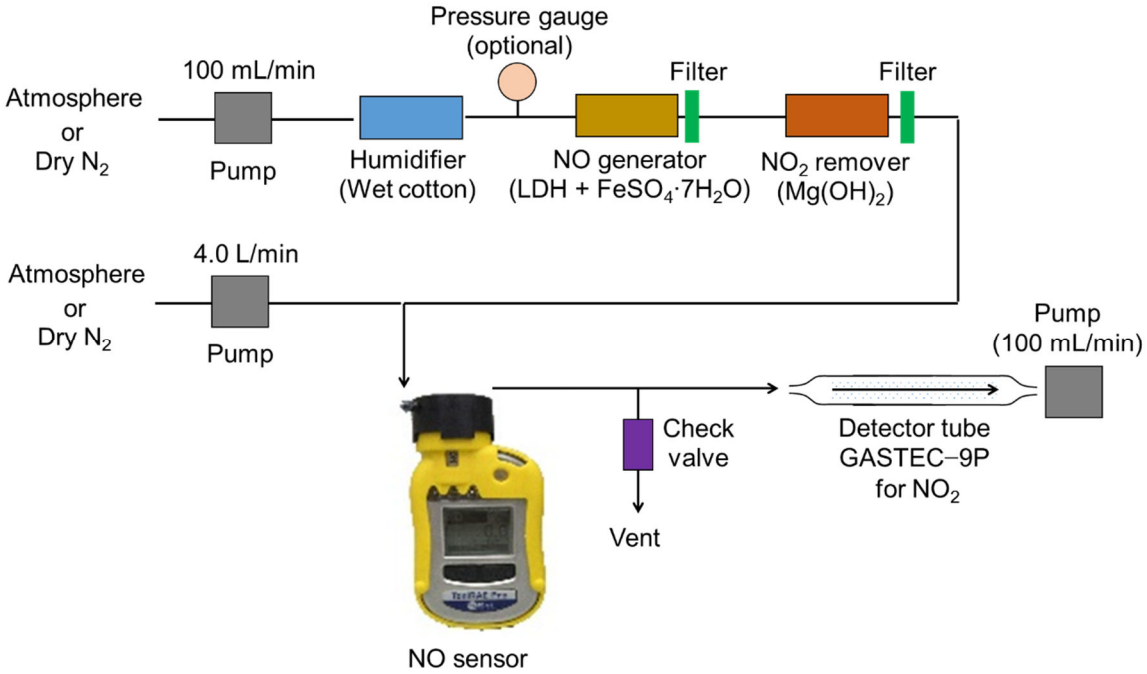

Scheme S5. Typical experimental set-up for monitoring NO and NO_2 released from $NaNO_2$-Mg/Al(3/1) and $FeSO_4 \cdot 7H_2O$ mixture. There is a little flow resistance in the NO generator and NO_2 remover due to the presence of powdery materials, and the barometric pressure before the NO generator is measured as 0.115 MPa (i.e., 0.014 MPa higher than ambient pressure (0.101 MPa)). The use of a larger amount of $Mg(OH)_2$ can be useful for further removal of NO_2, but this will increase the flow resistance.

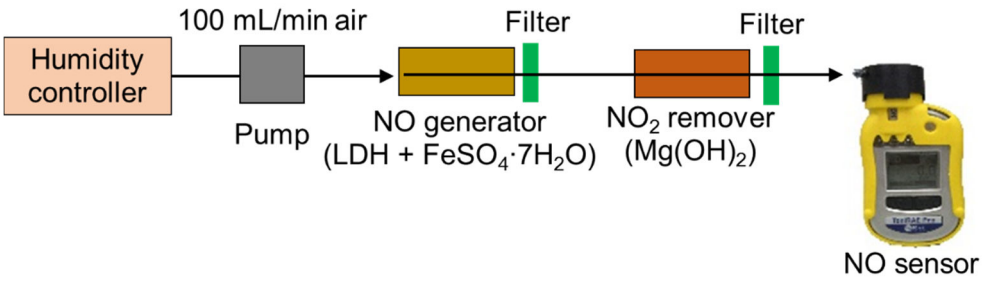

Scheme S6. Typical experimental set-up for monitoring NO released from $NaNO_2$-Mg/Al(3/1) and $FeSO_4 \cdot 7H_2O$ mixture. As a NO_2 remover, 4.0 g of $Mg(OH)_2$ loaded in a 12 mL plastic syringe was used.

S5.4. IR spectroscopy

NO demonstrates a characteristic IR spectrum at around 1800−1900 cm^{-1}. To exclude strong IR signals from CO_2 and H_2O, NO detection was performed under dry N_2, as shown in Scheme S7. N_2 humidified with wet cotton was delivered to the mixture of $NaNO_2$-Mg/Al(3/1) and $FeSO_4 \cdot 7H_2O$. NO_2 was removed with $Mg(OH)_2$, and then, water was removed with molecular sieve 3A for protecting the NaCl window. The dried N_2 involving NO was injected into a gas cell (GL Science, 10 cm optical length, NaCl windows), and the IR spectrum was monitored using an FT-IR spectrometer (Nicolet, NEXUS 670-FT-IR).

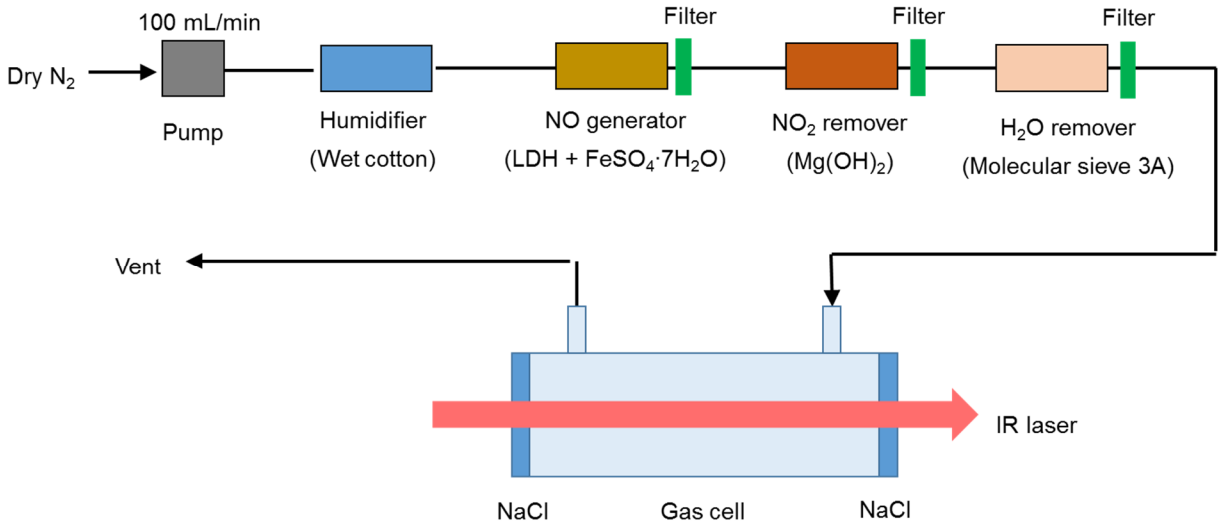

Scheme S7. Typical experimental set-up for monitoring NO by IR spectroscopy.

S5.5 Chemiluminescence

NO demonstrates characteristic chemiluminescent reaction with O_3 ($NO + O_3 \rightarrow NO_2 + O_2 + h\nu$), which is absolutely selective to NO over other NO_x. To avoid aerial oxidation of NO during the analysis, NO detection was performed under N_2, as shown in Scheme S8. N_2 humidified with wet cotton was delivered to $NaNO_2$-Mg/Al(3/1) and $FeSO_4 \cdot 7H_2O$ mixture. NO_2 was removed with $Mg(OH)_2$, and then, the analyte gas was injected into chemiluminescent NO/NO_x analyzer (Shimadzu, NOA-7000) equipped with a pretreatment chiller (for removal of water) and solenoid valve (for switching NO/NO_x detection modes).

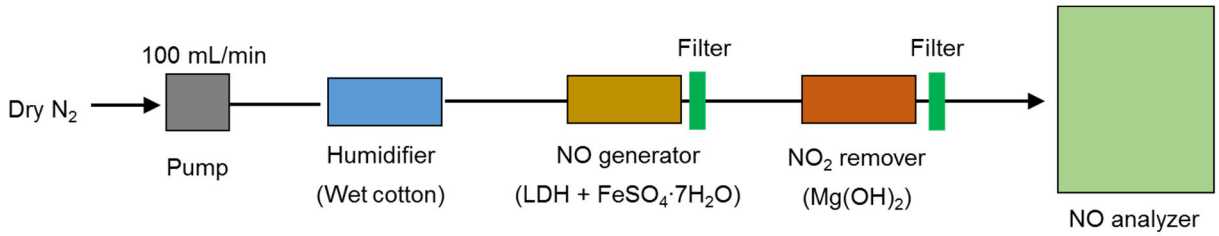

Scheme S8. Typical experimental set-up for monitoring NO by chemiluminescence NO analyzer.

S6. Additional miscellaneous data

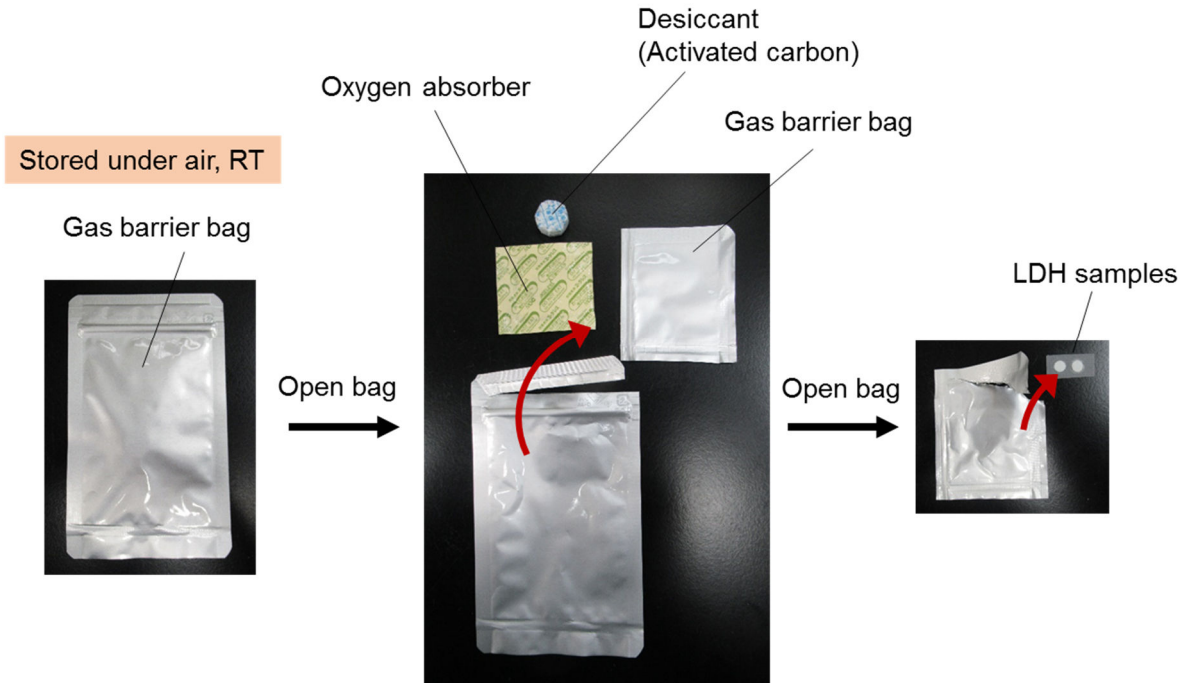

Fig. S1. Storage of gas-releasing LDH samples. Gas barrier bag (Lamizip® AL-D, Seisannipponsha, Ltd.), desiccant + activated carbon (DO1506, As One), and oxygen absorber (AGELESS®, Mitsubishi Gas Chemical) were used to isolate LDH samples from air.

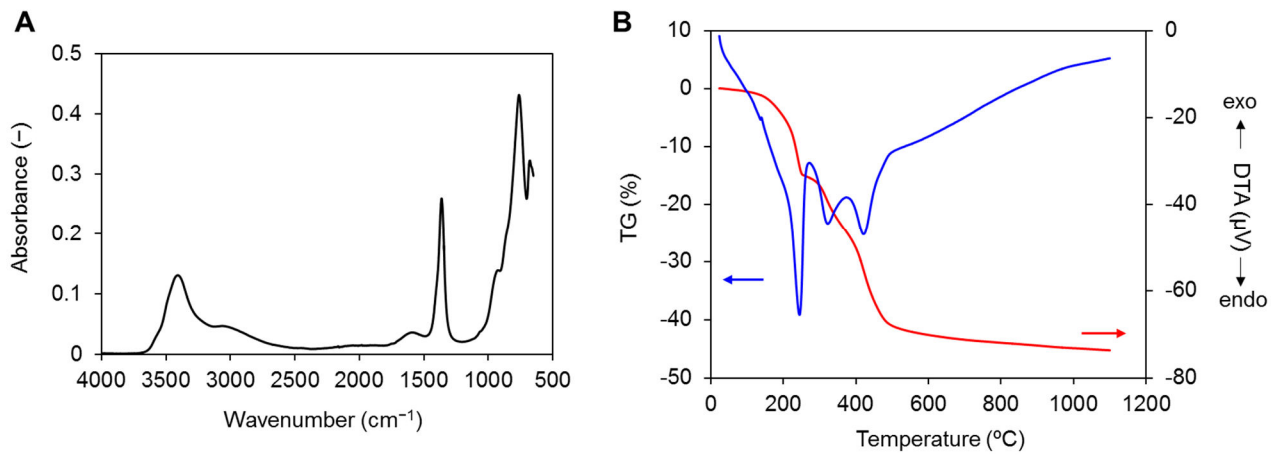

Fig. S2. IR spectrum (**A**) and TG-DTA profile (**B**) of as-prepared Na_2S-Mg/Al(2/1).

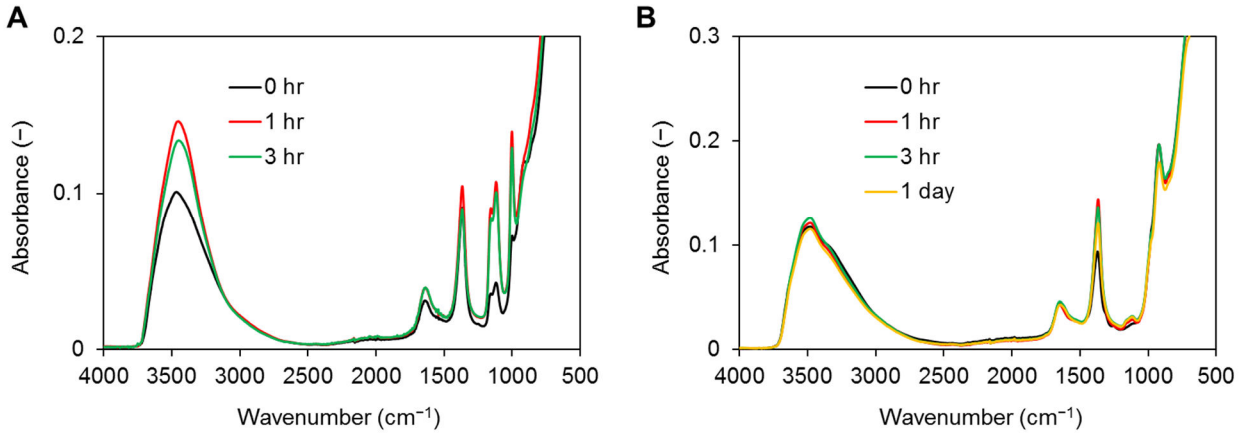

Fig. S3. IR spectra of (**A**) NaHS-Mg/Al(3/1) and (**B**) Na_2S-Mg/Al(3/1) after exposure to air.

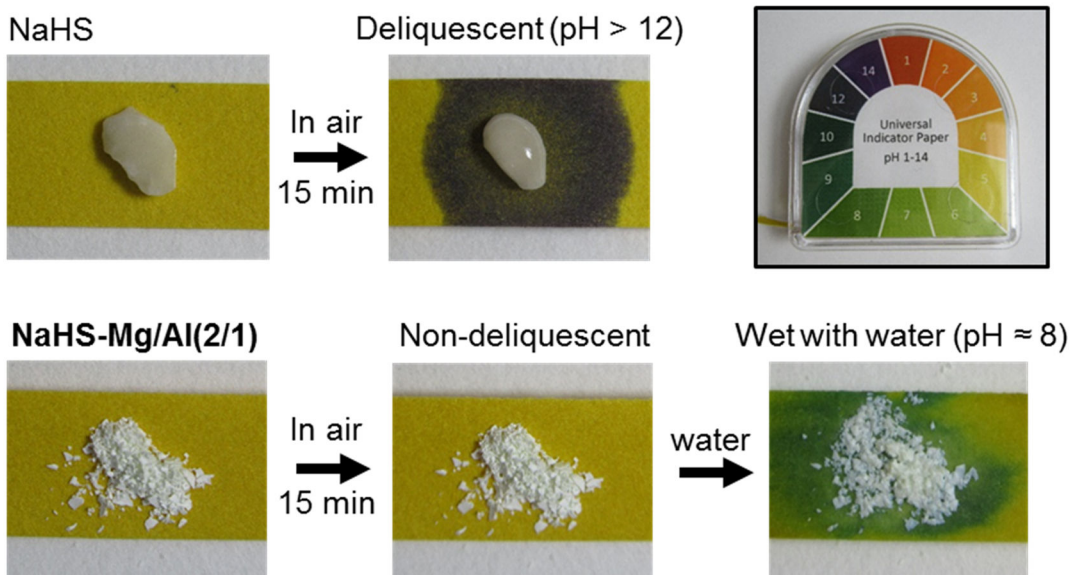

Fig. S4. Comparison of NaHS-Mg/Al(2/1) and NaHS in terms of handling safety (Note that aqueous solutions of NaHS and Na_2S are highly basic).

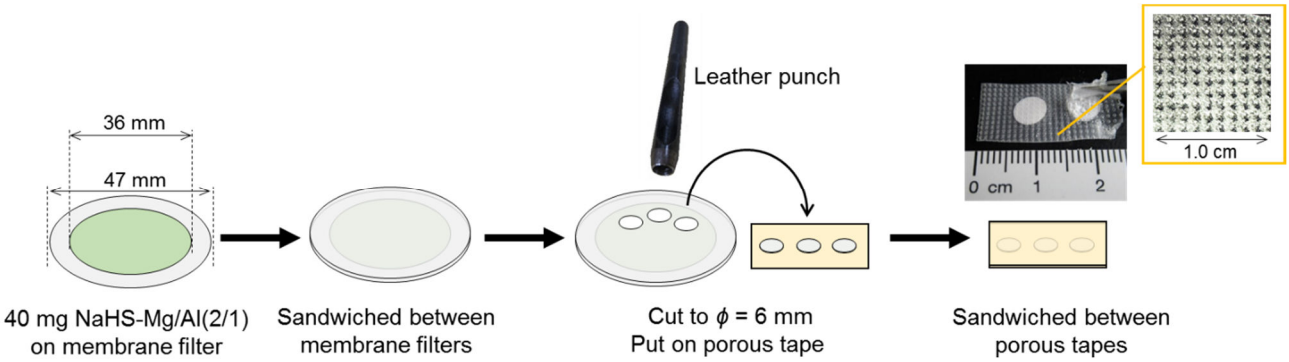

Fig. S5. Preparation of NaHS-Mg/Al(2/1) sandwiched between porous tapes (pore size = ~0.3 mm), yielding ~20 pieces of patches containing 1.1 mg NaHS-Mg/Al(2/1). Microscopy image of the porous tape is shown in the inset. Membrane filter (pore size = 0.2 μm) is identical to that utilized for filtration of LDHs in the syntheses.

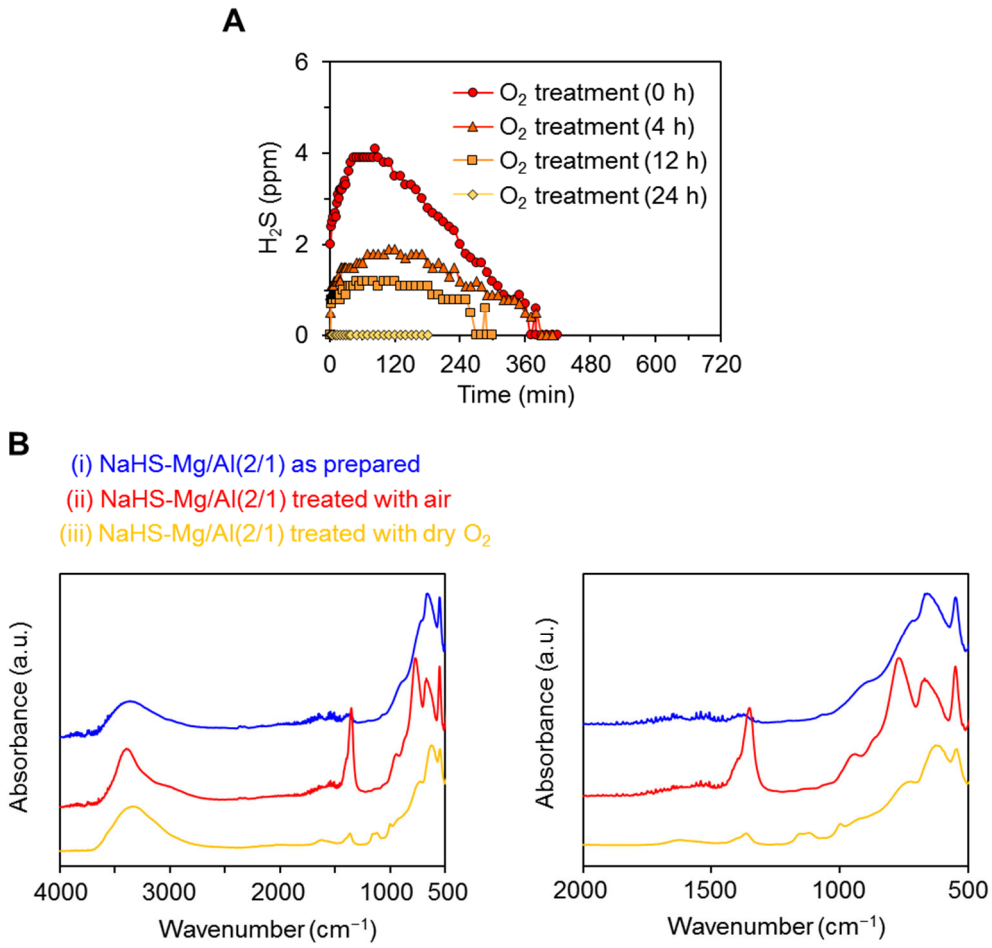

Fig. S6. (A) H_2S release profiles after treatment with pure O_2. Two patches of NaHS-Mg/Al(2/1) (1.1 mg × 2) sandwiched between the porous tapes were evaluated under the standard flow condition. **(B)** IR spectra of NaHS-Mg/Al(2/1) in the forms of (i) as-prepared, (ii) after treatment with air for 24 h, and (iii) after treatment with dry O_2 for 24 h.

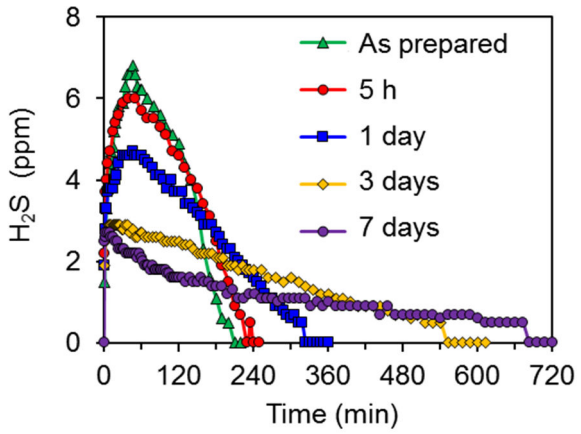

Fig. S7. Aging effect of NaHS-Mg/Al(2/1) under thermal treatment. Samples kept in gas barrier bag (Fig. S1) were heated at 60 °C in an electric oven, whose interior was purged with dry N_2. Two patches of NaHS-Mg/Al(2/1) (1.1 mg × 2) sandwiched between porous tapes were evaluated under the standard flow condition.

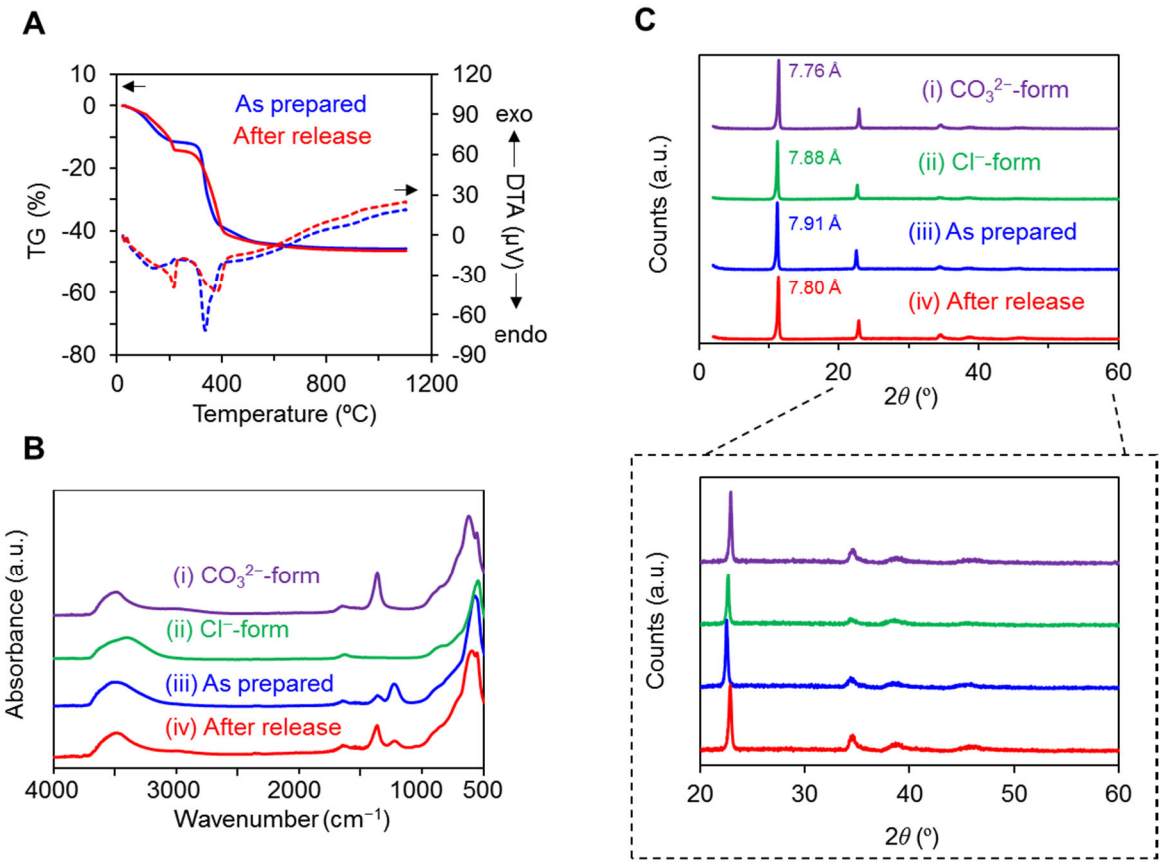

Fig. S8. Characterization of HNO_2-releasing LDHs. TG-DTA profiles (**A**), IR spectra (**B**), and XRD patterns and basal spacing (**C**) of $NaNO_2$-Mg/Al(3/1) in the forms of as-prepared and after treatment with exhaled-breath for two weeks. For comparison, IR spectra and XRD patterns of CO_3^{2-}-Mg/Al(3/1) and Cl^--Mg/Al(3/1) are also shown.

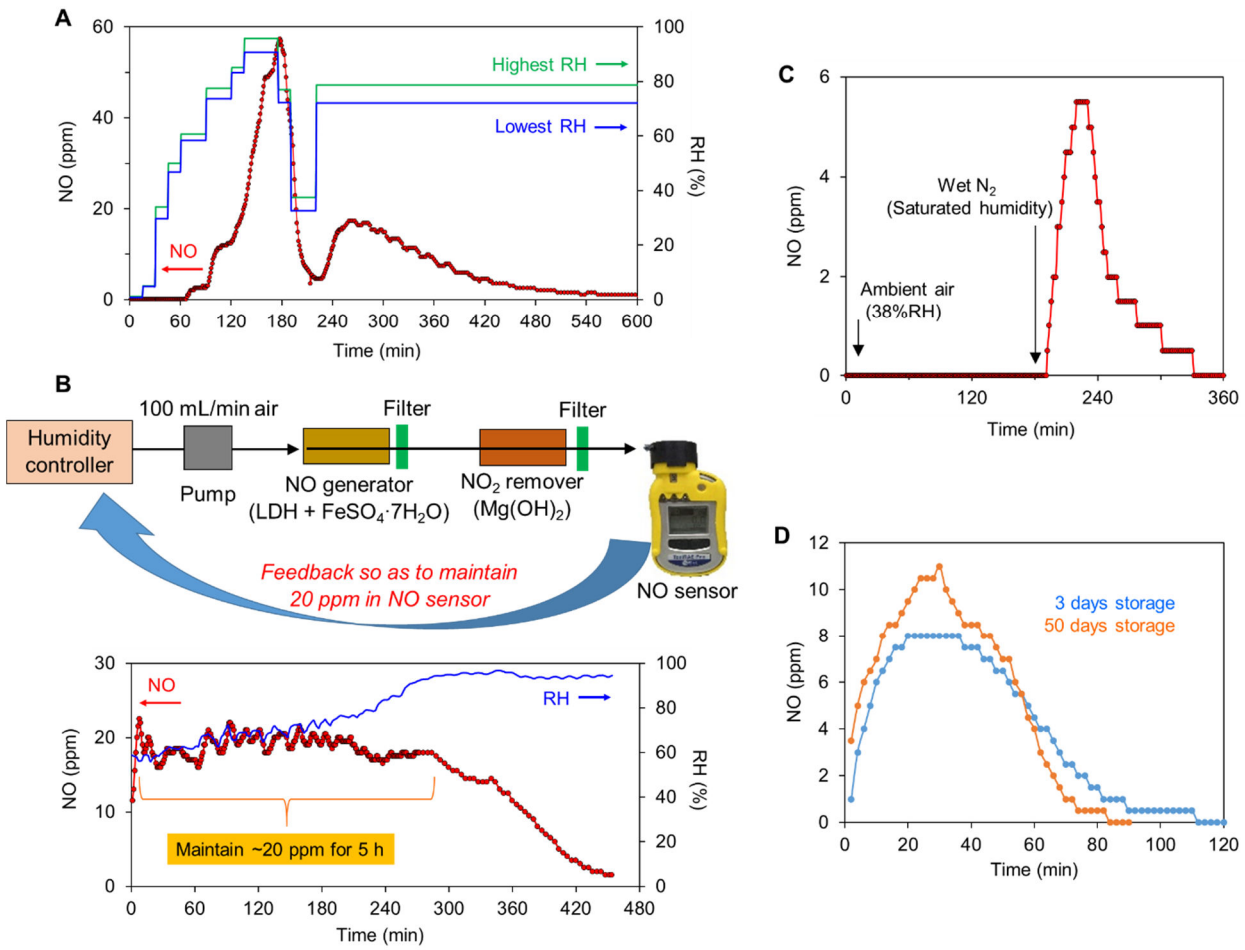

Fig. S9. (**A**) Release of NO from $NaNO_2$-Mg(3/1) (20 mg) and $FeSO_4 \cdot 7H_2O$ (0.2 g) mixture under air flow (100 mL/min) with variable humidity (0−95%RH). See Scheme S6 for the experimental set-up. The NO concentration was lower than the limit of detection of the electrochemical sensor (<0.5 ppm) when the relative humidity of air was lower than 60%. In contrast, if RH was increased by more than 60%, NO release was initiated. Humidity was occasionally changed (shown as steps), and the highest and lowest RHs during each step are shown in the graph. (**B**) Manipulating NO concentration by combining NO sensor and humidity controller. Humidity of air delivered to NO generator was adjusted (operated manually) such that the NO sensor maintained a value of 20 ppm. Mixture of $NaNO_2$-Mg(3/1) (20 mg) and $FeSO_4 \cdot 7H_2O$ (0.2 g) was used. (**C**) Release of NO from mixture of $NaNO_2$-Mg(3/1) (50 mg) and $FeSO_4 \cdot 7H_2O$ (0.5 g). See Scheme S5 for experimental set-up. The concentration of NO was lower than the limit of detection of the electrochemical sensor (<0.5 ppm) when ambient air (38%RH, 100 mL/min) was applied to the mixtures during the initial 3 h (note that NO was diluted with 4.0 L/min air). In contrast, the mixture started to release detectable amount of NO (>0.5 ppm) when wet N_2 (100 mL/min) was applied, indicating that humidity plays a critical role in NO generation. (**D**) Release of NO from $NaNO_2$-Mg(3/1) (50 mg) after 3 or 50 days storage. $NaNO_2$-Mg(3/1) was kept in a screw bottle (purged with dry N_2), and opened just before mixing with $FeSO_4 \cdot 7H_2O$ (0.5 g). See Scheme S5 for experimental set-up, where 100 mL/min ambient air (RH = 69%) and 4.0 L/min dry N_2 were utilized.

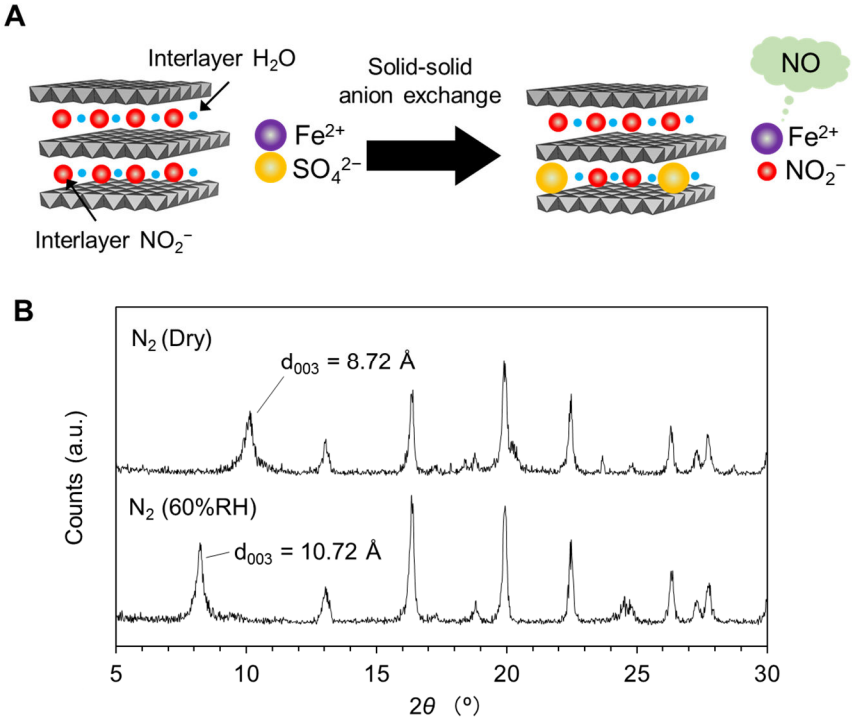

Fig. S10. (**A**) Proposed solid–solid state anion-exchange mechanism in $NaNO_2$-Mg(3/1) and $FeSO_4 \cdot 7H_2O$ mixture. Consequently, Fe^{2+} and NO^{2-} directly interacted (in other words, self-reactive $Fe^{II}(NO_2)_2$ was formed), leading to release of NO ($NO_2^- + Fe^{2+} + H_2O \rightarrow Fe^{3+} + 2OH^- + NO$). (**B**) XRD pattern of $NaNO_2$-Mg(3/1) and $FeSO_4 \cdot 7H_2O$ mixture after NO release, showing basal spacing (d_{003}) characteristic to SO_4^{2-}-type LDH (including response to humidity).

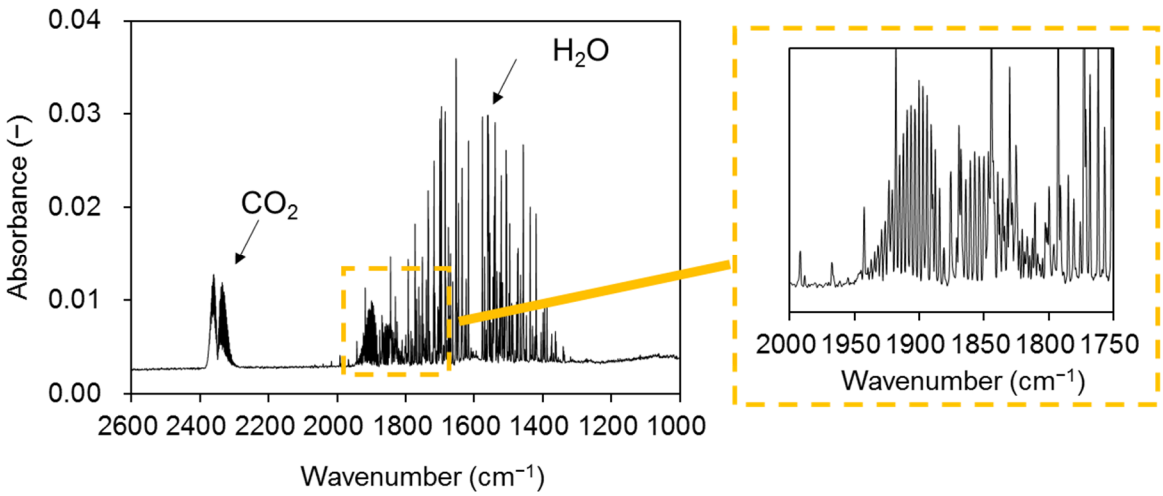

Fig. S11. IR spectrum of NO released from $NaNO_2$-Mg(3/1) (100 mg) and $FeSO_4 \cdot 7H_2O$ (1.0 g) mixture under wet N_2 (100 mL/min). NO was purified with $Mg(OH)_2$ (for removal of NO_2) and molecular sieve 3A (for removal of H_2O) before being injected into the gas cell (optical length = 10 cm, NaCl window). Note that neither N_2O (appear around 2200 cm^{-1}) nor NO_2 (appear around 1600 cm^{-1}) are observed in the spectrum. See Scheme S7 for experimental details.

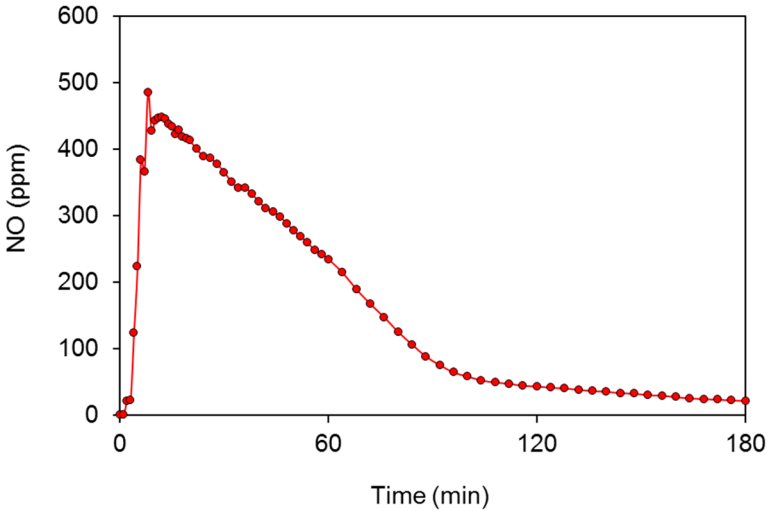

Fig. S12. Concentration of NO under N_2 flow (100 mL/min) monitored by chemiluminescent NO/NO_x analyzer. Mixture of $NaNO_2$-Mg(3/1) (100 mg) and $FeSO_4 \cdot 7H_2O$ (1.0 g) was used. See Scheme S8 for experimental details.

S7. Quantification of HS^- involved in LDH

The chemical formula of NaHS-Mg/Al(2/1) (prepared from 40 mg LDH and 36.6 mg $NaHS{\cdot}nH_2O$) was investigated by combing various analyses. First, H_2S release from 20 mg NaHS-Mg/Al(2/1) under standard flow condition (air, 50%RH, 100 mL/min, 20 °C) was monitored using electrochemical sensors, and the total amount of released H_2S was estimated to be 42.4 μmol based on the integration of the plot (Fig. S13A). After complete release of H_2S (applying standard flow condition for 24 h), TG-DTA profile of NaHS-Mg/Al(2/1) was measured from RT to 1100 °C under air (Fig. S13B). In addition, EDS spectra of NaHS-Mg/Al(2/1) before and after TG-DTA analysis were measured to determine the atom ratio of Mg, S, and Cl against Al (see Fig. S13C for typical spectra). Thus, NaHS-Mg/Al(2/1) before TG-DTA analysis showed Mg/Al = 2.05, S/Al = 0.0386, Cl/Al = 0.158, and that after TG-DTA analysis showed Mg/Al = 2.06, S/Al = 0.0125, Cl/Al = not detected.

Taking TG-DTA profile, EDS, and charge-balancing into account, the chemical formula of calcined NaHS-Mg/Al(2/1) at 1102 °C was estimated as $Mg_{2.05}AlO_{3.54}(SO_4)_{0.0125}$. Besides, the tentative chemical formula of NaHS-Mg/Al(2/1) at 230 °C was set as $Mg_{2.05}Al(OH)_{6.1}(S_2O_3)_{0.0193}(Cl)_{0.158}(CO_3)_x$, where the amounts of Mg, S_2O_3, and Cl were determined based on the EDS result. The amount of (OH) was determined to maintain the charge balance of the layer (i.e., $Mg_{2.05}Al(OH)_{6.1}$) as +1. Based on the difference of mass in the TG-DTA profile of $Mg_{2.05}AlO_{3.54}(SO_4)_{0.0125}$ (1102 °C, 5.106 mg) and $Mg_{2.05}Al(OH)_{6.1}(S_2O_3)_{0.0193}(Cl)_{0.158}(CO_3)_x$ (230 °C, 7.990 mg), the amount of carbonate was determined as $x = 0.372$. Then, based on the difference of mass in the TG-DTA profile of $Mg_{2.05}Al(OH)_{6.1}(S_2O_3)_{0.0193}(Cl)_{0.158}(CO_3)_{0.372}$ (230 °C, 7.990 mg) and $Mg_{2.05}Al(OH)_{6.1}(HS)_{0.0386}(Cl)_{0.158}(CO_3)_{0.372}{\cdot}yH_2O$ (RT, 9.14 mg), the amount of hydrated water was determined as $y = 1.73$. Thus, the chemical formula of NaHS-Mg/Al(2/1) after H_2S release under air was confirmed.

Tentative chemical formula of NaHS-Mg/Al(2/1) before H_2S release was set as $Mg_{2.05}Al(OH)_{6.1}(HS_{non\text{-}emissive})_{0.0386}(HS_{emissive})_z(Cl)_{0.158}(OH)_w{\cdot}1.73H_2O$. It was assumed that emissive $(HS_{emissive})_z$ and $(OH)_w$ will be replaced with $(CO_3)_{0.372}$ after exposure to air; thus, $(z + w)/2 = 0.372$. Then, the value of z was determined, such that 20 mg of NaHS-Mg/Al(2/1) released 42.4 μmol of H_2S. Consequently, the chemical formula of NaHS-Mg/Al(2/1) before release of H_2S was determined as $Mg_{2.05}Al(OH)_{6.1}(HS_{non\text{-}emissive})_{0.0386}(HS_{emissive})_{0.507}(Cl)_{0.158}(OH)_{0.237}{\cdot}1.73H_2O$. Thus, majority (~93%) of HS^- involved in NaHS-Mg/Al(2/1) was released as H_2S, and ~7% was non-emissive due to aerial oxidation to $S_2O_3^{2-}$ and/or polysulfide. In the given chemical formula, 1 mg of NaHS-Mg/Al(2/1) contains 0.073 mg sulfur (S) source as an atom.

As an alternative approach, the amount of HS^- involved in NaHS-Mg/Al(2/1) was directly determined by the methylene blue method. In the globe box (dry N_2), 10 mg of NaHS-Mg/Al(2/1) was dispersed in 10 mL of degassed deionized water containing 60 mg of Na_2CO_3 (excess to HS^-). The suspension was sonicated for 2 min to disperse LDH, and the anion-exchange reaction between HS^- and CO_3^{2-} was promoted (LDH is known to show high affinity to CO_3^{2-}). Within 6 or 24 h of the

anion exchange, ~10 mg (1 or 2 drops) of the suspension (the weight was exactly measured by balance) was added to 1.5 mL of degassed deionized water. Then, the concentration of sulfur (as HS^-/S^{2-}) in the solution was analyzed by the methylene blue method using a commercially available test kit (WAK-S, Kyoritsu Chemical-Check Lab., Corp.). The UV-vis absorption spectrum of the blue solution was measured at 25 °C using a 1 mm quartz cell, and the concentrations of sulfur (as HS^-/S^{2-}) involved in the suspension after 6 h and 24 h anion-exchange reaction were estimated to be 0.069 mg/mL and 0.072 mg/mL, respectively, based on the calibration curve prepared separately (Fig. S13D). This result indicates that ~0.07 mg of sulfur atom (as HS^-/S^{2-}) was released from 1 mg of NaHS-Mg/Al(2/1), which agrees with the aforementioned chemical formula of NaHS-Mg/Al(2/1) (i.e., 0.073 mg sulfur atom is involved in 1 mg NaHS-Mg/Al(2/1)).

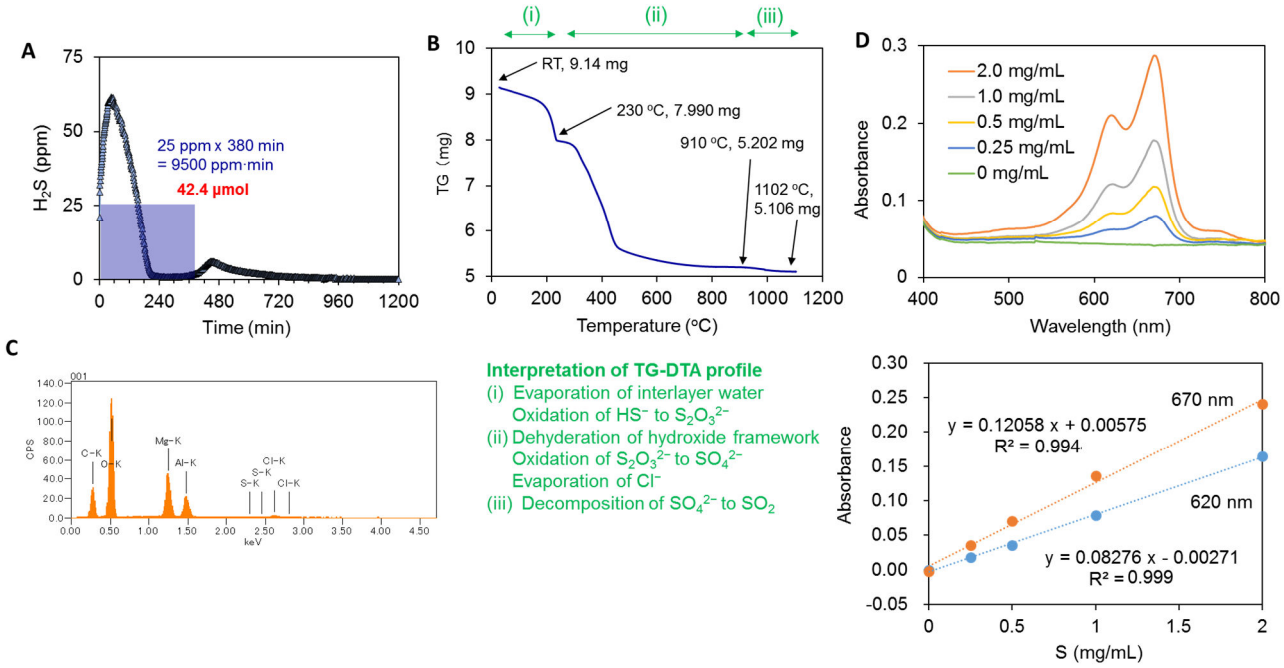

Fig. S13. (**A**) H_2S release profile of 20 mg of powdery NaHS-Mg/Al(2/1) under the standard flow condition. (**B**) TG-DTA profile of NaHS-Mg/Al(2/1) after complete release of H_2S. Interpretation of the profile is also shown. (**C**) Typical EDS spectra of NaHS-Mg/Al(2/1) after release of H_2S. At least four EDS spectra were averaged to determine the atom ratio. (**D**) Calibration curve of sulfur (as HS^-/S^{2-}) in water based on methylene blue method. Standard aqueous solution of Na_2S (0, 0.25, 0.5, 1.0, and 2.0 mg/mL) was prepared by dissolving 35.45 mg of freshly opened anhydrous Na_2S (Dojindo Laboratories) in degassed deionized water (7.27 mL). The standard solution (5 μL) was added to 5.0 mL of degassed deionized water, and then analyzed by a test kit (WAK-S, Range = 0.1−5 mg/L, Kyoritsu Chemical-Check Lab., Corp.). UV-vis absorption spectra of the solution were measured at 25 °C using a quartz cell with 1 mm optical length.

S8. Quantification of NO_2^- involved in LDH

The amount of NO_2^- involved in $NaNO_2$-Mg/Al(3/1) was quantified using the Griess reagent. We dispersed 10.2 mg of $NaNO_2$-Mg/Al(3/1) in 10 mL of degassed deionized water containing 30 mg of Na_2CO_3. The suspension was sonicated for 1 min to disperse LDH, and left for 30 min to promote anion exchange between NO_2^- and CO_3^{2-} (LDH is known to show high affinity to CO_3^{2-}). The suspension (1 mL) was centrifuged to precipitate LDH, and then, 5 μL of the supernatant solution was added to 0.5 mL of the aqueous solution of Griess reagent (40 mg/mL).

The UV-vis absorption spectrum of the stained solution was measured at 25 °C using 1 mm quartz cell, and the NO_2^- concentration involved in the supernatant solution was estimated to be 2.74 mM based on the calibration curve prepared separately (Fig. S14). This result indicates that 1.26 mg of NO_2^- was released from 10.2 mg of $NaNO_2$-Mg/Al(3/1), and the weight fraction of NO_2^- in $NaNO_2$-Mg/Al(3/1) was 12.4 wt.%. Note that the use of 60 mg of Na_2CO_3 for anion exchange yielded the same result. In addition, it was confirmed that the anion-exchange reaction was completed in 30 min as the same result was obtained after 2 h of the anion-exchange reaction.

Besides, SEM-EDS analysis showed that Al:Cl ratio in $NaNO_2$-Mg/Al(3/1) was approximately 1:0.09. Assuming that the molecular formula of $NaNO_2$-Mg/Al(3/1) was $Mg_3Al(OH)_8(Cl^-_{0.09}, NO_2^-{}_{0.91})\cdot 2H_2O$, according to the general formula of LDHs with neutral charge balance, the weight fraction of NO_2^- in the formula was 13.2 wt.%. The weigh fraction of NO_2^- determined by the Griess reagent method (i.e., 12.4 wt.%) was close to this value, and thus, the chemical formula of $NaNO_2$-Mg/Al(3/1) is close to $Mg_3Al(OH)_8(Cl^-_{0.09}, NO_2^-{}_{0.91})\cdot 2H_2O$.

It is estimated that 100 mg of $Mg_3Al(OH)_8(Cl^-_{0.09}, NO_2^-{}_{0.91})\cdot 2H_2O$ contains 0.287 mmol of NO_2^-, which corresponds to the release of 357 ppm NO for 180 min under 100 mL/min flow. The actual amount of NO released from LDHs was about half of the expected value (e.g., see Fig. S12).

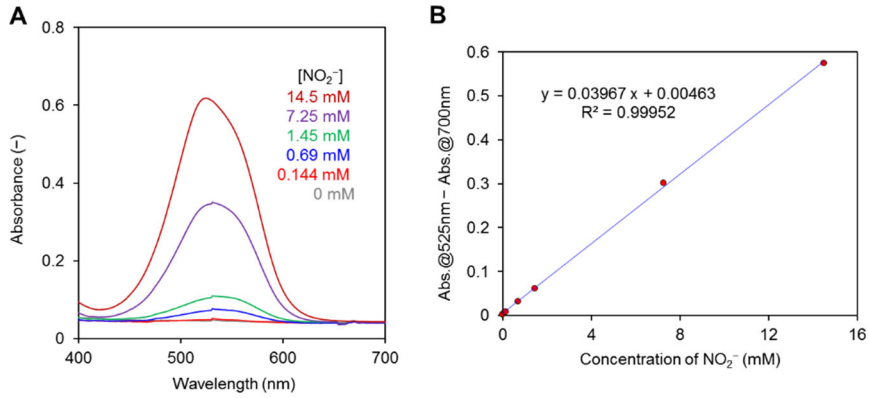

Fig. S14. (**A**) UV-vis absorption spectra of Griess reagent responding to NO_2^-. 5 μL of $NaNO_2$ solution (0, 0.144, 0.69, 1.45, 7.25, and 14.5 mM) in water was added to 0.5 mL of aqueous solution of Griess reagent (40 mg/mL), wherein the Griess reagent was in large excess to NO_2^-. A quartz cell with 1 mm optical length was used for the measurement. (B) Calibration curve of NO_2^-, showing liner correlation between NO_2^- concentration and absorbance of Griess reagent.

S9. Additional discussion on H_2S release profile

The H_2S release profiles of NaHS-Mg/Al(2/1) under air form a parabolic curve (e.g., Fig. 2I), where the H_2S concentration gradually increases and then decreases. If H_2S generation simply follows eq. 1 in Fig. 1B ($2[HS^-]_{LDH} + CO_2 + H_2O \rightarrow 2H_2S\uparrow + [CO_3^{2-}]_{LDH}$), the H_2S concentration solely depends on the amount of $2[HS^-]_{LDH}$ (until the concentrations of CO_2 and H_2O are constant). Thus, the initial concentration of H_2S should be the highest and its release curve should be a simple decay type.

It was found that the use of methanol (MeOH) in the synthesis of NaHS-Mg/Al(2/1) (in reaction and washing processes) provided a decay curve in the release profile of H_2S with high initial concentration (Fig. S15A). In contrast, if NaHS-Mg/Al(2/1) prepared in MeOH was washed with degassed deionized water several times, the initial concentration of H_2S was dramatically decreased. This result suggests that the interlayer HS^- located at the edge of layers was replaced with OH^- when washed with water (note that pK_a values of H_2S and H_2O are close) (Fig. S15B). As aerial CO_2 and H_2O also diffuse into the LDH interlayer from the edge, H_2S release will be low until CO_2 completes reaction with OH^- ($2[OH^-]_{LDH} + CO_2 \rightarrow H_2O + [CO_3^{2-}]_{LDH}$). Then, aerial CO_2 gradually reacts with HS^- located inside the LDH layer, resulting in a parabolic curve. The anion distribution model shown in Fig. S15B also explains the aging effect of NaHS-Mg/Al(2/1) in H_2S release (e.g., Fig. 3I) as homogenization of the interlayer layer anion, recovering to a decay curve with reduced concentration.

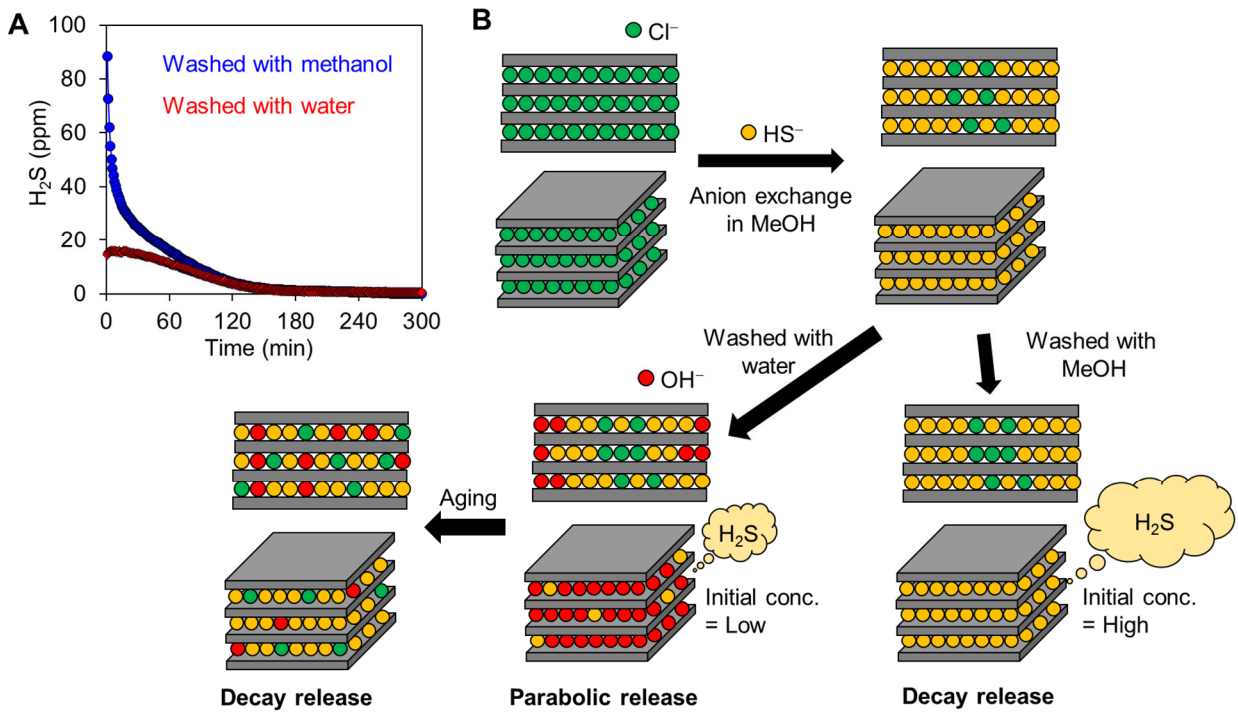

Fig. S15 (**A**) H_2S release profile (under the standard flow condition) of 5.0 mg of NaHS-Mg(2/1) prepared in MeOH. After completing two days reaction in MeOH, solid materials were filtrated on the membrane filter, and then washed with either methanol or water. (**B**) Plausible anion distribution model in LDHs for explaining their release profiles of H_2S.